CRE in the COX-2 promoter. NO appears to accelerate existing intracellular signals rather than generating new signaling, and thus may promote the growth and survival of tumor cells. These novel results suggest that additional studies on the role of NO in carcinogenesis may be warranted and that iNOS should potentially be re-evaluated as a molecular target for cancer prevention and treatment.

Materials and methods

Cell culture

HNSCC cells line SNU-1041 was obtained from the Korean Cell Line Bank (Seoul National University, Seoul, Korea) (Chung *et al.*, 2000), while HNSCC cell line PCI-13 was obtained from the Pittsburgh Cancer Institute (University of Pittsburgh, PA, USA) (Heo *et al.*, 1989). We additionally used gastric cancer cell line SNU-668 (Song *et al.*, 2001) and HeLa. All cells were cultured in DMEM or RPMI-1640 media supplemented with 10 mg/ml gentamicin and 10% fetal bovine serum (FBS). Cells were maintained at 37°C in a humidified, 5% CO_2, 95% air atmosphere and routinely subcultured using trypsin-EDTA (0.25% w/v). All cell culture reagents were obtained from Gibco BRL (Grand Island, NY, USA), unless otherwise stated.

Chemicals

SNAP (NO donor), db-cGMP, PMA, L-NAME (universal NOS inhibitor), AG (specific iNOS inhibitor), LPS and EGF were obtained from Sigma Chemical Co. (St Louis, MO, USA). ODQ (soluble guanylate cyclase (sGC) inhibitor), SB202190 (p38 MAPK inhibitor), SP600125 (JNK inhibitor), U0126 (ERK inhibitor), PD153015 (ERK inhibitor), 2′,3′-Dideoxyadenosine (2-3-DDA, PKA inhibitor), 2-[1-93-Dimethylaminopropyl]-1H-indol-3-yl)-3-(1H-indol-3-yl)-maleimide (Bisindolylmaleimide I, PKC inhibitor), Bisindolylmaleimide IX (Ro-31-8220, PKC inhibitor) and Rp-8-pCPT-cGMPs (PKG inhibitor) were obtained from Calbiochem (La Jolla, CA, USA). 1400W (specific iNOS inhibitor) was obtained from Cayman (Ann Arbor, MI, USA). Most chemicals were utilized according to the provided suggestion (IC50 and references), with the exception of SNAP and 1400W, which were applied according to our previous optimization study results (Park *et al.*, 2003).

COX-2 promoter activity assay

The COX-2 promoter constructs (−1432/+59(L), −327/+59 (S), KBM, ILM, CRM, KBM+ILM, KBM+CRM, ILM+CRM, and Triple M) were generated as previously described (Inoue *et al.*, 2000). The PGL2-Basic control vector was purchased from Promega (Madison, WI, USA), and the pSV-β galactosidase control vector was a kind gift from Dr Yung-Jue Bang (Cancer Research Institute, Seoul National University, Seoul, Korea). Cells were seeded at 10^5/well in 12-well culture plates and grown to 70–80% confluence in complete growth media containing 10% FBS. Cells were cotransfected with 0.5 μg COX-2 promoter construct and 0.5 μg pSV-β galactosidase control vector using Lipofectamine Plus according to the manufacturer's instructions (Life Technologies, Gaithersburg, MD, USA). After 4 h, medium containing 10% FBS was added and cells were incubated for an additional 20 h. Subsequently, cells were incubated in serum-free medium for 24 h and then treated for 18 h with the NO donor and/or other chemicals as indicated. Luciferase activity was measured using a TR717 Microplate Luminometer with a Bioluminescent Reporter Gene Assay kit, according to the manufacturer's instructions (Tropix, Bedford, MA, USA). The pGL2-Basic vector without insert was used as the negative control in transfection experiments. Luciferase activity was normalized according to that of β-galactosidase.

Gel shift assay

Gel shift experiments were performed using a gel shift assay system according to the manufacturer's instructions (Promega, Madison, WI, USA). Cells were harvested and nuclear extracts were prepared. We designed and synthesized double-stranded oligonucleotides containing the CRE site of the COX-2 promoter (5′-AAA CAG TCA TTT CGT CAC ATG GGC TTG-3′). Oligonucleotides containing the consensus sequences of the CREB (5′-AGA GAT TGC CTG ACG TCA GAG AGC TAG-3′), AP-1 (5′-CGC TTG ATG AGT CAG CCG GAA-3′) and NF-κB (5′-AGT TGA GGG GAC TTT CCC AGG-3′) sites were obtained from Promega (Madison, WI, USA) and used as unlabeled competitors. The complementary oligonucleotides containing the CRE of the COX-2 promoter were annealed in 20 mM Tris-Cl (pH 7.4), 50 mM NaCl, 10 mM $MgCl_2$, and 1 mM dithiothreitol. Annealed oligonucleotides were phosphorylated at the 5′-end with [γ-^{32}P]ATP and T4 polynucleotide kinase. The binding reaction was performed by incubating 5 μg of nuclear proteins with 5× binding buffer (50 mM Tris-Cl (pH 7.5), 20% glycerol, 5 mM $MgCl_2$, 2.5 mM EDTA, 2.5 mM dithiothreitol, 250 mM NaCl and 0.25 mg/ml poly (dI-dC)) in a final volume 9 μl for 10 min at room temperature. Then, 1 μl of the labeled oligonucleotide was added to the reaction mixture and incubated for 20 min at room temperature. For the competition assay, unlabeled oligonucleotides containing the CRE of COX-2, or the CREB, AP-1 or NF-κB consensus sequences were used. The samples were incubated with anti-CREB, anti-ATF-2, anti-c-jun or anti-c-fos antibodies for 1 h, followed by addition of ^{32}P-labeled oligonucleotides containing the CRE site of COX-2. Samples were electrophoresed on a Novex 6% DNA retardation gel (Invitrogen). The gel image was transferred to an imaging plate (BAS-MP 2040S, Fuji Photo Film Co., Tokyo, Japan), and the degree of binding was calculated based on hybridization signals measured with a bio-imaging analyser (FRA2000 system, Fuji Photo Film Co., Tokyo, Japan).

TF activation assay

The fusion trans-activator plasmids (pFA-ATF-2, pFA2-CREB, and pFA2-cJun) consisting of the DNA binding domain of Gal4 (residue 1–147) and the trans-activation domains of ATF-2, CREB or c-jun were purchased from Stratagene (La Jolla, CA, USA). pFC2-dbd, which contains only the DNA binding domain of Gal4 (residue 1–147), was used as the negative control. We performed experiments according to the manufacturer's instructions.

Protein extraction and Western blot analysis

Cultured cells were rinsed with PBS, suspended in lysis buffer (0.5% NP40, 50 mM Tris-Cl, 150 mM NaCl, 1 mM dithiothreitol, 1% Triton X-100, 1% sodium deoxycholate, 0.1% SDS, 1 mM EDTA, 1 mM phenylmethylsulfonyl fluoride, 0.1 μM aprotinin, and 1 μM pepstatin A), and incubated at 4°C for 30 min. The cell lysates were then centrifuged at 13 000 r.p.m. for 20 min at 4°C, and then appropriate amount of supernatant (determined by protein assay) was mixed with 4× sample loading buffer and denatured for 10 min at 70°C. The

denatured protein samples were fractionated on 4–12% NuPAGE gels (Invitrogen, Carlsbad, CA, USA), transferred onto nitrocellulose membranes (Schleicher & Schuell, Dachen, Germany) and incubated with Tris-buffered saline containing 0.1% Tween-20 and 5% nonfat dry milk. The membranes were then incubated with anti-COX-2, anti-p38, anti-phospho-p38, anti-JNK, anti-phospho-JNK, anti-c-fos (all from Santa Cruz Biotechnology, Santa Cruz, CA, USA), monoclonal anti-α-tubulin (Sigma Chemical Co., St Louis, MO, USA), anti-CREB, anti-phospho-CREB, anti-ATF-2, anti-phospho-ATF-2, anti-c-jun or anti-phospho-c-jun (all from Cell Signaling Technology, Beverly, MA, USA) for 2 h at room temperature or overnight at 4°C. Membranes were then washed (4 × 15 min) with 1 × TBS-T and incubated with horseradish peroxidase-conjugated secondary antibody (Pierce, Rockford, IL, USA) for 1 h. Immunoreactive proteins were visualized by development with the lumi-light Western blotting substrate (Roche Diagnostics GmbH, Mannheim, Germany) and exposure to X-ray film.

Statistical analysis

The data are presented as the mean ± standard deviation (s.d.) of triplicates, or as a representative of three separate experiments. Levels of significance were determined between treated and untreated groups by two-sided Student's *t*-test.

Abbreviations

NO, nitric oxide; iNOS, inducible nitric oxide synthase; COX-2, cyclooxygenase-2; CRE, cAMP-response element; sGC, soluble guanylate cyclase; PGE_2, prostaglandin E_2; HNSCC, head and neck squamous cell carcinoma; MAPK, mitogen-activated protein kinase; ERK, extracellular signal-regulated kinase; JNK, c-Jun NH_2-terminal kinase; CREB, cAMP response element-binding protein; ATF-2, activating transcription factor-2; AP-1, activator protein-1; PKA, cAMP-dependent protein kinase; PKC, protein kinase-C; PKG, protein kinase G.

Acknowledgements

We thank Dr Lee Jung Weon (Cancer Research Institute, Seoul National University, Seoul, Korea) for helpful discussion. This work was supported in part by a Korea Research Foundation Grant (KRF-2002-041-E00134) and by BK21 project for Medicine, Dentistry and Pharmacy, Korea.

References

Bogdan C. (2001). *Trends Cell Biol.*, **11**, 66–75.
Browning DD, Mcshane MP, Marty C and Ye RD. (2000). *J. Biol. Chem.*, **275**, 2811–2816.
Chabot-Fletcher M. (1996). *Pharmacol. Rev. Commun.*, **8**, 317–324.
Chan G, Boyle JO, Yang EK, Zhang F, Sachs PG, Shah JP, Edelstein D, Soslow RA, Koki AT, Woerner BM, Masferrer JL and Dannenberg AJ. (1999). *Cancer Res.*, **59**, 991–994.
Chung PS, Rhee CK, Kim KH, Paek W, Chung J, Paiva MB, Eshraghi AA, Castro DJ and Saxton RE. (2000). *Laryngoscope*, **110**, 1312–1316.
Coffery RJ, Hawkey CJ, Damstrup L, Graves-Deal R, Daniel VC, Dempsey PJ, Chinery R, Kirkland SC, DuBois RN, Jetton TL and Morrow JD. (1997). *Proc. Natl. Acad. Sci. USA*, **94**, 657–662.
Gallo O, Masini E, Morbidelli L, Franchi A, Fini-Storchi I, Vergari WA and Ziche M. (1998). *J. Natl. Cancer Inst.*, **90**, 587–596.
Guo YS, Hellmich MR, Wen XD and Townsend Jr CM. (2001). *J. Biol. Chem.*, **276**, 22941–22947.
Habib A, Bernard C, Lebret M, Creminon C, Esposito B, Tedgui A and Maclouf J. (1997). *J. Immunol.*, **158**, 3845–3851.
Han JA, Kim JI, Ongusaha PP, Hwang DH, Ballou LR, Mahale A, Aaronson SA and Lee SW. (2002). *EMBO J.*, **21**, 5635–5644.
Heo DS, Snyderman C, Gollin SM, Pan S, Walker E, Deka R, Barnes EL, Johnson JT, Herberman RB and Whiteside TL. (1989). *Cancer Res.*, **49**, 5167–5175.
Howe LR, Crawford HC, Subbaramaiah K, Hassell JA, Dannenberg AJ and Brown AM. (2001). *J. Biol. Chem.*, **276**, 20108–20115.
Inoue H, Tanabe T and Umesono K. (2000). *J. Biol. Chem.*, **275**, 28028–28032.
Lee DW, Sung MW, Park SW, Seong WJ, Roh JL, Park BJ, Heo DS and Kim KH. (2002). *Anticancer Res.*, **22**, 2089–2096.
Liaudet L, Soriano FG and Szabo C. (2000). *Crit. Care Med.*, **28** (Suppl), N37–N52.
Liu Y, Borchert GL and Phang JM. (2004). *J. Biol. Chem.*, **279**, 18694–18700.
Luque I and Gelinas C. (1997). *Semin. Cancer Biol.*, **8**, 103–111.
Nose F, Ichikawa T, Fujiwara M and Okayasu I. (2002). *Am. J. Clin. Pathol.*, **117**, 546–551.
Pai R, Soreghan B, Szabo IL, Pavelka M, Baatar D and Tarnawski AS. (2002). *Nat. Med.*, **8**, 289–293.
Park SW, Lee SG, Song SH, Heo DS, Park BJ, Lee DW, Kim KH and Sung MW. (2003). *Int. J. Cancer*, **107**, 729–738.
Park YK, Nesterova M, Agrawal S and Cho-Chung YS. (1999). *J. Biol. Chem.*, **274**, 1573–1580.
Posadas I, Terencio MC, Guillen I, Ferrandiz ML, Coloma J, Paya M and Alcaraz MJ. (2000). *Naunyn-Schied. Arch. Pharmacol.*, **361**, 98–106.
Salvemini D, Misko TP, Masferrer JL, Seibert K, Currie MG and Needleman P. (1993). *Proc. Natl. Acad. Sci. USA*, **90**, 7240–7244.
Sheng H, Shao J, Washington MK and DuBois RN. (2001). *J. Biol. Chem.*, **276**, 18075–18081.
Slice LW, Bui L, Mak C and Walsh JH. (2000). *Biochem. Biophys. Res. Commun.*, **276**, 406–410.
Son HJ, Kim YH, Park DI, Kim JJ, Rhee PL, Paik SW, Choi KW, Song SY and Rhee JC. (2001). *J. Clin. Gastroenterol.*, **33**, 383–388.
Song SH, Jong HS, Choi HH, Inoue H, Tanabe T, Kim NK and Bang YJ. (2001). *Cancer Res.*, **61**, 4628–4635.
Stadler J, Harbrecht BG, DiSilvio M, Curran RD, Jordan ML, Simmons RL and Billiar TR. (1993). *J. Leukocyte Biol.*, **53**, 165–172.
Subbaramaiah K, Norton L, Gerald W and Dannenberg AJ. (2002). *J. Biol. Chem.*, **277**, 18649–18657.
Sun Y, Tang XM, Elizabeth HM, Kuo T and Sinicrope FA. (2002). *Cancer Res.*, **62**, 6323–6328.
Surh YJ, Chun KS, Cha HH, Han SS, Keum YS, Park KK and Lee SS. (2001). *Mutat. Res.*, **480–481**, 243–268.
Tamura M, Sbastian S, Yang S, Gutates B, Ferrer K, Sasano H, Okamura K and Bulun SE. (2002). *J. Biol. Chem.*, **277**, 26208–26216.

Tanabe T and Tohnai N. (2002). *Prostaglandins Other Lipid Mediators*, **68–69**, 95–114.
Tang Q, Chen W, Gonzales MS, Finch J, Inoue H and Bowden GT. (2001). *Oncogene*, **20**, 5164–5172.
Tsai AL, Wei C and Kulmacz RJ. (1994). *Arch. Biochem. Biophys.*, **313**, 367–372.
Vadlamudi R, Mandal M, Adam L, Steinbach G, Mendelsohn J and Kumar R. (1999). *Oncogene*, **18**, 305–314.
Wink DA, Vodovotz Y, Laval J, Laval F, Dewhirst MW and Mitchell JB. (1998). *Carcinogenesis*, **19**, 711–721.
Xu XM, Tang JL, Chen X, Wang LH and Wu KK. (1997). *J. Biol. Chem.*, **272**, 6943–6950.

THE JOURNAL OF BIOLOGICAL CHEMISTRY VOL. 280, NO. 37, pp. 32379–32388, September 16, 2005

T-oligo Treatment Decreases Constitutive and UVB-induced COX-2 Levels through p53- and NFκB-dependent Repression of the COX-2 Promoter*[S]

Received for publication, March 24, 2005, and in revised form, July 14, 2005 Published, JBC Papers in Press, July 26, 2005, DOI 10.1074/jbc.M503245200

Vaneeta Marwaha[‡1], Ya-Hui Chen[‡1,2], Elizabeth Helms[‡], Simin Arad[‡], Hiroyasu Inoue[§], Evelyn Bord[¶], Raj Kishore[¶], Raffi Der Sarkissian[‖], Barbara A. Gilchrest[‡3], and David A. Goukassian[‡4]

From the [‡]Departments of Dermatology and [‖]Division of Facial Plastic and Reconstructive Surgery, Boston University School of Medicine, Boston, Massachusetts 02118, [§]Nara Women's University, Nara 630-8506, Japan and [¶]Division of Cardiovascular Research, St. Elizabeth's Medical Center, Boston, Massachusetts 02135

Chronically irradiated murine skin and UV light-induced squamous cell carcinomas overexpress the inducible isoform of cyclooxygenase (COX-2), and COX-2 inhibition reduces photocarcinogenesis in mice. We have reported previously that DNA oligonucleotides substantially homologous to the telomere 3′-overhang (T-oligos) induce DNA repair capacity and multiple other cancer prevention responses, in part through up-regulation and activation of p53. To determine whether T-oligos affect COX-2 expression, human newborn keratinocytes and fibroblasts were pretreated with T-oligos or diluent alone for 24 h, UV-irradiated, and processed for Western blotting. In both cell types, T-oligos transcriptionally down-regulated base-line and UV light-induced COX-2 expression, coincident with p53 activation. In fibroblasts with wild type versus dominant negative p53 ($p53^{WT}$ versus $p53^{DN}$), T-oligos decreased constitutive expression of a COX-2 reporter plasmid by >50%. We then examined NFκB, a known positive regulator of COX-2 transcription. In $p53^{WT}$ but not in $p53^{DN}$ fibroblasts and in human keratinocytes, T-oligos decreased readout of an NFκB promoter-driven reporter plasmid and decreased NFκB binding to DNA. After T-oligo treatment and subsequent UV irradiation, binding of the transcriptional co-activator protein p300 to NFκB was decreased, whereas binding of p300 to p53 was increased. Human skin explants provided with T-oligos had markedly decreased COX-2 immunostaining both at base-line and post-UV light, coincident with increased p53 immunostaining. We conclude that T-oligos transcriptionally down-regulate COX-2 expression in human skin via activation and up-regulation of p53, at least in part by inhibiting NFκB transcriptional activation. Decreased COX-2 expression may contribute to the observed ability of T-oligos to reduce photocarcinogenesis.

Nonmelanoma skin cancer accounts for well over 1 million cases of human malignancy annually in the United States, and the incidence continues to rise (1–3). The major initiator and promoter of skin cancer is UVB radiation (4, 5). Among the contributing effects of UVB radiation on skin are the formation of cyclobutane-pyrimidine dimers and pyrimidine (6-4) photoproducts (6, 7), which lead to mutations in key regulatory genes (8), epidermal hyperplasia (9, 10) allowing for expansion of mutated clones (11), immunosuppression (12, 13), and inflammation (14, 15).

One way inflammation in particular is thought to affect carcinogenesis is by promoting epidermal hyperplasia and proliferation through production of cytokines and various second messengers such as prostaglandin E_2 (16). The major enzyme responsible for the UVB-induced prostaglandin synthesis is cyclooxygenase-2 (COX-2),[5] the inducible isoform of the cyclooxygenase enzyme (17) that carries out the rate-limiting step of prostaglandin and thromboxane production (18–20). COX-2 has been shown to be overexpressed in numerous human malignancies, including colon, lung, and breast cancers (21–24). In relation to skin cancer, UVB irradiation increases both mRNA and protein levels of COX-2 in human keratinocytes (25). Recent studies have shown increased COX-2 expression in human skin in response to acute UVB exposure as well as increased COX-2 expression in human and murine tumors that were induced by chronic UVB exposure (26, 27). Furthermore, specific inhibitors of Cox-2 such as celecoxib have been shown not only to decrease tumorigenesis and increase tumor latency in hairless mice models (28) but also to decrease tumor growth in hairless mice with pre-existing UVB-induced tumors (29). In addition, Cox-2-overexpressing transgenic mice have shown dramatic increase in predisposition to tumor development in tumor promotion studies (30).

Given the evidence implicating COX-2 in tumorigenesis and tumor maintenance, methods to decrease COX-2 levels in response to UVB irradiation are currently being investigated as a promising means of cancer prevention. Known inhibitors of COX-2 include estrogens, antioxidants, and p53 (31–33). The presence of active p53 in particular has been shown to decrease both the mRNA and protein levels of Cox-2 in mouse embryo fibroblasts (33). In a study of head and neck squamous cell carcinomas (SCCs), tumors with mutated p53 showed higher COX-2 protein levels than tumors expressing wild type (WT) p53 (34). Evidence thus suggests that activating p53 and thereby reducing COX-2 expression in the absence of DNA damage might decrease photocarcinogenesis and inhibit growth of established tumors.

In mammalian cells, telomeres are tandem repeats of a short DNA sequence, 5′-TTAGGG-′ and its complement that cap chromosome

* This work was supported in part by National Institutes of Health Grant RO-1 CA105156-01 and by the Herzog Foundation. The costs of publication of this article were defrayed in part by the payment of page charges. This article must therefore be hereby marked "*advertisement*" in accordance with 18 U.S.C. Section 1734 solely to indicate this fact.

[S] The on-line version of this article (available at http://www.jbc.org) contains Figs. S1–S7.

[1] Both authors contributed equally to this work.

[2] Supported by the Veterans General Hospital, Kaohsiung, Taiwan. Present address: Dept. of Dermatology, Veterans General Hospital, Kaohsiung, Taiwan.

[3] To whom correspondence may be addressed: Dept. of Dermatology, Boston University School of Medicine, 609 Albany St., Boston, MA 02118. Tel.: 617-638-5541; Fax: 617-638-5515; E-mail: bgilchre@bu.edu.

[4] To whom correspondence may be addressed: Dept. of Dermatology, Boston University School of Medicine, 609 Albany St., Boston, MA 02118, Tel.: 617-638-5541; Fax: 617-638-5515; E-mail: dgoukass@bu.edu.

[5] The abbreviations used are: COX-2, cyclooxygenase-2; pTT, thymidine dinucleotide; WT, wild type; DN, dominant negative; SCC, squamous cell carcinoma; T-oligos, telomere homolog oligonucleotide (repeats of TTAGGG); EMSAs, electrophoretic mobility shift assays; TBPs, TATA-binding proteins; ATM, ataxia telangiectasia mutated.

ends and form a large loop structure (35). The loop is held closed by an ~100–400-base single-stranded 3′-overhang that inserts into the proximal double-stranded telomere and is secured by binding proteins, particularly telomere repeat binding factor (TRF2) (36). Disruption of this loop structure by sequestration of the binding protein with a dominant negative construct ($TRF2^{DN}$) leads to exposure of the 3′-overhang sequence (repeats of TTAGGG), digestion of the overhang, and signaling through ATM and p53 that induces DNA damage responses (37). We have found that providing cultured cells with DNA oligonucleotides substantially homologous to the telomere sequence, which we term T-oligos, mimics telomere loop disruption, leading to ATM/p53 signaling (38) and the DNA damage-like responses of senescence (39) or apoptosis (40) but apparently without disruption of the loop or other effects on genomic DNA (40). Because these 2–11-base T-oligos concentrate rapidly in the nucleus (40, 41), we hypothesize that T-oligos are interpreted by the cell as indicating telomere loop disruption, specifically exposure of the otherwise concealed 3′-overhang sequence (38–40), and hence initiate signaling for DNA damage-like responses without antecedent DNA damage.

T-oligos with 100% telomere homology, delivered at a sufficiently high dose, elicit predominantly "end point" cancer protective responses such as apoptosis or proliferative senescence that remove cells, particularly malignant cells, from the proliferative pool (40, 42, 43). However, it is also possible to provide cells with a less than maximal DNA damage signal by reducing the T-oligo dose and/or employing a shorter or less telomere-homologous oligonucleotide. Under these circumstances, it is possible to observe transient reversible cell cycle arrest (44), increased melanogenesis in pigment cells and intact skin (44–46), release of immunomodulatory cytokines from keratinocytes associated with abrogation of allergic contact sensitization or elicitation in intact skin (47, 48), enhanced rate and accuracy of DNA repair both *in vitro* and *in vivo* (49–51), and decreased mutation rate and tumor development *in vivo* (51). Moreover, malignant cells appear to undergo apoptosis or senescence more readily in response to a given T-oligo at a given dose than do their normal nontransformed cellular counterparts (42, 43).

In the present study, we show that treatment with either of two oligonucleotides with partial telomere homology decreases constitutive and UVB-induced COX-2 levels in cultured human fibroblasts, human skin explants, and intact murine skin. These responses are shown to occur at least in part through up-regulation and activation of p53, leading to transcriptional repression of COX-2 promoter activity. We propose that in addition to the previously reported protective DNA damage responses, treatment with T-oligos may also decrease the cutaneous inflammatory response through inhibition of COX-2 expression, a possible additional means of reducing photocarcinogenesis.

EXPERIMENTAL PROCEDURES

Cell Culture—Primary human neonatal fibroblast and keratinocytes cultures were established as described (49, 50). Cells were incubated at 37 °C in 5% CO_2. Cell lines permanently (retroviral transfection) expressing WT p53 (R2FWT) or dominant negative p53 (R2FDD) (52–54) were the generous gift from Dr. Jim Rheinwald (Department of Dermatology, Harvard Skin Disease Research Center, Harvard Medical School, Boston) and were maintained in R2F medium containing 42.5% Dulbecco's modified Eagle's medium, 42.5% F-12, 15% calf serum, and 0.1% epidermal growth factor at 37 °C in 5% CO_2.

Oligonucleotides—Previous experiments have shown that 100 μM of thymidine dinucleotide (pTT), representing one-third of the telomere repeat, and 40 μM of pGAGTATGAG (p9-mer), a 55% homologous sequence, are roughly bioequivalent concentrations for the elicitation of UV mimetic responses (49, 50, 55, 56), including p53 up-regulation and activation. Oligonucleotides (pTT and p9-mer) were synthesized with phosphodiester linkage by Midland Certified Reagent (Midland, TX) and diluted in H_2O to form a 2 mM stock. This stock solution was then diluted in the appropriate culture medium to 100 or 40 μM, respectively, and added to culture dishes for use in experiments. Cells and skin explants were provided T-oligos only once at time 0 and then harvested at intervals, according to the design of the specific experiment. All experiments were conducted using both pTT and p9-mer and gave identical results with either T-oligo.

UVB Irradiation—After 48 h of incubation in medium containing pTT, p9-mer, or diluent alone, cells or skin explants were placed in phosphate-buffered saline and irradiated through the plastic culture dish cover by using a solar simulator (Spectral Energy Corp., Westwood, NJ). The 1-kilowatt xenon arc lamp (XMN-1000-21; Optical Radiation Corp., Azuza, CA) irradiance was adjusted to 5×10^{-5} watts/cm^2, and dishes were exposed to 15 mJ/cm^2 as measured with a research radiometer fitted with a UV light probe at 285 ± 5 nm (model IL1700 A; International Light, Newburyport, MA) (56, 57), a protocol that exposes cells to a spectrum of light resembling terrestrial sunlight (58). Sham-irradiated cultures were handled identically, except that they were shielded with aluminum foil during irradiation. After irradiation, cells were given fresh medium lacking T-oligos.

Western Blot Analysis—Total cellular proteins were collected as described previously (46). Concentrations were determined by the Bio-Rad method, and 50 μg of protein were run in each lane on a 10% denaturing SDS-polyacrylamide gel. Proteins were then transferred to a nitrocellulose membrane. Antibody reactions were performed with the following antibodies: phospho-$p53^{Ser15}$ (Cell Signaling Technology, Beverly, MA), p53 DO-1, COX-2, NFκB/p65, and actin (all from Santa Cruz Biotechnology, Santa Cruz, CA). Western blot analysis was then performed as described (46).

Electrophoretic Mobility Shift Assays—Electrophoretic mobility shift assays (EMSAs) using consensus p53 and NFκB oligonucleotides (Santa Cruz Biotechnology) and 5 μg of nuclear protein from variously treated cells were carried out as described previously (59). Reactions were electrophoresed on 5% nondenaturing polyacrylamide gels, dried, and processed for autoradiography. For competition experiments, 50–100-fold excess of unlabeled DNA were added to the reaction 20 min before the addition of radiolabeled probe.

Transfection Studies—Constructs containing the full-length phPES2(−1432/+59) human Cox-2 promoter, a deletion construct of phPES2(−327/+59), and an NFκB binding region site-specific mutant of phPES2(−327/+59) attached to a luciferase reporter (60, 61) or an NFκB reporter plasmid (Promega Corp., Madison, WI) were employed. The pGL2 vector used for cloning the reporter construct was obtained from Promega (pGL2-Basic, Promega Corp., Madison, WI) and was used as an empty vector control. A plasmid containing *Renilla* luciferase (pRL-CMV, Promega Corp., Madison, WI) was co-transfected as a control for transfection efficiency. R2FWT and R2FDD cells were plated in 35-mm tissue culture dishes and incubated in R2F medium overnight to reach 50–60% confluence the next day. Cells were then transfected using the Lipofectamine 2000 (Invitrogen) according to the manufacturer's protocol. Two μg of plasmid DNA were co-transfected with 0.15 μg of the *Renilla* luciferase plasmid in each dish. After 4–6 h of transfection, cells were supplemented either with R2F medium alone (diluent) or R2F medium with 40 μM p9-mer or 100 μM pTT. Cells were then incubated for 24 and 48 h at 37 °C in 5% CO_2 before harvesting for dual-luciferase assay. Promoter activity was then assayed using a dual-luciferase reporter assay system (Promega Corp., Madison, WI) according to the manufacturer's protocol. Firefly luciferase values were corrected for transfection efficiency according to *Renilla* luciferase values

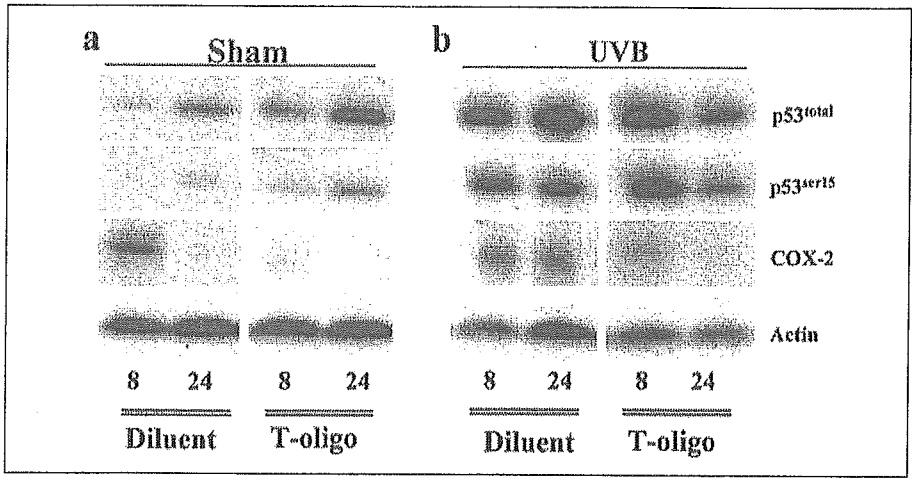

FIGURE 1. **T-oligo pretreatment up-regulates and activates p53 and down-regulates constitutive and UV light-induced COX-2 expression.** Human fibroblasts were pretreated once with diluent or T-oligo (p9-mer 40 μM; pTT data not shown) for 48 h. *a*, paired dishes were then sham-irradiated and harvested after 8 and 24 h and processed for Western blot analysis to evaluate the expression of COX-2, $p53^{total}$, $p53^{Ser15}$, and actin (loading control). Between 8 and 24 h, T-oligo pretreatment down-regulated constitutive COX-2 expression, which was inversely related to up-regulation of $p53^{total}$ and $p53^{Ser15}$ levels. These experiments were repeated three times with similar results. *b*, paired dishes were then UVB-irradiated with 15 mJ/cm^2, harvested, and then processed as for *a*. In diluent-treated UV light-irradiated samples, $p53^{total}$ and $p53^{Ser15}$ levels increased from 8 to 24 h, whereas in T-oligo-treated UV light-irradiated cells, $p53^{total}$ and $p53^{Ser15}$ expression was greater at 8 h. This earlier and higher up-regulation and activation of p53 in T-oligo-treated UV light-irradiated cells were accompanied by a striking decrease at 8 h and virtually complete inhibition of UV light-induced COX-2 expression in T-oligo-treated *versus* diluent-treated control cells. Similar results were obtained in three independent experiments with no difference between p9-mer and pTT results.

and revealed minimal differences in transfection efficiency among dishes. Luciferase activity was then expressed as percent of diluent value, setting diluent as 100%.

Immunoprecipitation and Immunoblotting—Cell lysates were precleaned with protein G-Sepharose beads for 2 h at 4 °C. Then 100 μg of total cell proteins were incubated with 2 μg of monoclonal p300 antibodies (GeneTex® Inc., San Antonio, TX), followed by the addition of protein G-Sepharose beads. The immunoprecipitated products were then subjected to SDS-PAGE and Western blot analysis as described (62). After transferring proteins to nitrocellulose membrane antibody reactions were performed with NFκB (p65) antibodies and p53 (DO-1) (both from Santa Cruz Biotechnology).

Human Skin Explant Studies—Human skin fragments from healthy donors (aged 56 ± 15 years, mean ± S.D.) were brought to the laboratory within 30 min after excision during plastic or facial reconstructive surgery. After removing subcutaneous fat and deep dermis, skin was cut into 5 × 5-mm squares and placed in 60-mm tissue culture dishes. Paired skin explants were then incubated in either medium alone or medium supplemented with 100 μM pTT or 40 μM p9-mer for 24 h. Medium consisted of Dulbecco's modified Eagle's medium with 10% calf serum plus KBM-2 with growth factors (50/50 v/v). The skin explants were then irradiated with a single dose of 30 mJ/cm^2 UVB. One set was sham-irradiated as a negative control. For each treatment, one explant was harvested immediately after UVB irradiation. The dishes were then re-fed with fresh medium lacking T-oligos, and explants were harvested at 6, 18, and 24 h after UVB irradiation. Harvested skin was snap-frozen at −80 °C in OCT medium for later processing.

Immunohistochemistry and Immunofluorescence—Snap-frozen human skin explants were processed for staining by cutting 4–6-μm sections and fixing them in acetone for 10 min at −20 °C. COX-2 staining was performed using the Ultravision Detection System (TQ-015-HA, Labvision Corp., Fremont, CA) according to manufacturer's protocol. Primary antibodies used included anti-COX-2 (Santa Cruz Biotechnology), human anti-p53 DO-7 (DakoCytomation, Carpinteria, CA), and anti-phospho-$p53^{Ser15}$ (Cell Signaling Technology, Beverly, MA). For the p53 DO-7 and $p53^{Ser15}$ stainings, sections were blocked in 10% goat normal serum in Tris-buffered saline for 15 min at room temperature and then incubated with primary antibody overnight at 4 °C. Sections were then washed in Tris-buffered saline three times for 5 min each before being incubated with the appropriate fluorescein isothiocyanate-labeled secondary antibody at 37 °C for 45 min. Finally, sections were washed as before and mounted with Vectashield mounting medium containing 4′,6-diamidino-2-phenylindole to visualize nuclei and were stored at −20 °C. We delineated ≈10-μm × 1-mm areas using computer-assisted image analysis and counted $p53^{total}$ and $p53^{Ser15}$ (+) nuclei in the epidermis. For each time point we analyzed an average of three randomly selected visual fields of $p53^{total}$ and $p53^{Ser15}$-stained epidermis from three to five donors per treatment condition. To avoid bias all counts were done by a single investigator for whom all samples were blinded by another investigator.

Statistical Analysis—Difference in protein expression, Cox-2 promoter activity, and $p53^{total}$ and $p53^{Ser15}$ (+) nuclei in T-oligo *versus* control-treated samples were analyzed by the analysis of variance post hoc analysis using the StatView statistical program (SAS Institute, Gary, NC). Groups were considered different when $p < 0.05$ (50).

RESULTS

T-oligo Pretreatment Down-regulates Base-line and UVB-induced COX-2 Protein Levels That Coincide with Up-regulation and Activation of p53 Levels—The effect of T-oligo pretreatment on constitutive and UV light-induced levels of COX-2 and p53 was examined by Western blot analysis (Fig. 1), and results were confirmed by densitometric analysis of the blots (Fig. S1). In diluent-treated sham-irradiated cells, the constitutive $p53^{total}$ and $p53^{Ser15}$ levels were negligible at 8 h and moderately increased 24 h later (Fig. 1*a* and Fig. S1, *a* and *b*), consistent with approaching confluence of the cultures.[6] Reciprocally, COX-2 was constitutively expressed in diluent-treated sham-irradiated samples at 8 h and decreased by 24 h (Fig. 1*a* and Fig. S1*c*). In comparison, in T-oligo-treated sham-irradiated cells, COX-2 protein levels were strikingly lower at 8 h and virtually undetectable at 24 h, time points 56 and 72 h after T-oligo supplementation (Fig. 1*a* and Fig. S1*c*), suggesting that T-oligo treatment for 48 h down-regulates constitutive COX-2 levels in human fibroblasts. These decreases in COX-2 protein level were

[6] V. Marwaha, B. A. Gilchrest, and D. A. Goukassian, unpublished observations.

inversely related to the increases in both $p53^{total}$ and $p53^{Ser15}$ in T-oligo-treated sham-irradiated cells (Fig. 1*a* and Fig. S1, *a* and *b*).

UV irradiation up-regulated $p53^{total}$ and $p53^{Ser15}$ levels by 8 h and through 24 h and up-regulated COX-2 within 24 h, as reported previously (25, 50, 55), in diluent-treated cells (Fig. 1*b* and Fig. S1, *d–f*). T-oligo-treated cells also showed UV light-induced increases in $p53^{total}$ and $p53^{Ser15}$, with both sham- and UV light-induced levels markedly higher than in diluent-treated controls, as expected (55). As also expected if active p53 negatively regulates COX-2 levels, in T-oligo-treated cells COX-2 was virtually undetectable by 24 h after UVB (Fig. 1*b* and Fig. S1*f*), the time of maximal UV light-induced COX-2 protein expression reported by others (27, 63). After UV irradiation, maximal p53 induction and activation are reported to occur at ~2–24 h (depending on UV light dose) (64). Because T-oligo pretreatment appeared to accelerate the time of peak, UV light induction and activation of p53 as well as to increase the magnitude of p53 induction and activation (Fig. 1), we examined a more detailed time course, harvesting fibroblasts pretreated with T-oligo or diluent alone for 48 h immediately after UV irradiation and after 4, 6, 8, 16, and 24 h (Fig. S2). Consistent with our interpretation of the experiment shown in Fig. 1, diluent-pretreated cells showed peak phospho-$p53^{Ser15}$ induction at 6–8 h, with a return to base-line by 24 h, whereas T-oligo-pretreated cells had ~85% higher phospho-$p53^{Ser15}$ levels immediately post-irradiation and had tripled this induction within 4 h of an ~3-fold increase that gradually declined through 24 h (Fig. S2). Total p53, in contrast to activated p53, showed similar patterns in both T-oligo and diluent pretreated fibroblasts with substantial inductions by 4 h of post-UV light that declined only slightly by 24 h. However, in diluent-pretreated cells, $p53^{total}$ levels were far lower (~4-fold) of $p53^{total}$ levels in T-oligo-pretreated cells (Fig. S2). In combination, these data are consistent with a delayed direct effect of T-oligos on COX-2 expression, such as altered transcription rate subsequently reflected in protein levels. Alternatively or in addition, this may indicate involvement of an subsequent event downstream of p53 activation, such as p53-mediated inhibition of a known positive COX-2 transcriptional regulator, such as NFκB, NF-IL6, or AP1 (65–67).

T-oligo Pretreatment Down-regulates COX-2 through p53-dependent Repression of COX-2 Promoter—To evaluate further the involvement of p53 in T-oligo-induced down-regulation of COX-2 expression, we performed transient transfection studies using two isogenic fibroblast cell lines, one that expresses WT p53 (R2FWT) and one that is permanently transfected with dominant negative p53 (R2FDD) (52–54).

As shown by Western blot analysis and quantification by densitometry, R2FDD cells expressed higher constitutive levels of $p53^{total}$ and $p53^{Ser15}$ than R2FWT cells (~6- and or 40-fold, respectively), as expected (54), and showed virtually no T-oligo-induced up-regulation of either $p53^{total}$ or $p53^{Ser15}$ (Fig. 2*a* and Fig. S3a), whereas in R2FWT cells by 24 h T-oligo induced a more than 5-fold increase in $p53^{Ser15}$ and a 37% increase in $p53^{total}$ levels (Fig. 2*a* and Fig. S3*b*).

To verify that the p53 status of the cell lines had not changed over time in culture, we next evaluated T-oligo-induced p53 DNA binding activity. EMSA showed that in T-oligo-treated R2FDD cells, consensus sequence binding was minimal and did not increase over time, whereas in contrast binding in R2FWT cells was far higher as early as 8 h and was maximal by 24 h (Fig. 2*b*). These data confirm the reported p53 status in the R2FWT *versus* R2FDD cells.

The transcription factor NFκB is a known positive regulator of *COX-2* gene expression (68). Because recent reports indicate that activation of p53 by various stimuli inhibits NFκB activity (69, 70), we next evaluated NFκB DNA binding to its consensus sequence after T-oligo treatment. In both R2FWT and R2FDD cells that received T-oligos in fresh medium, NFκB binding decreased between 1.5 and 8 h and then increased again by 16 h (Fig. 2*c*), consistent with the known serum-mediated bi-phasic increase in NFκB activity (71–73). However, by 24 h, the time of maximal p53 activation in R2FWT cells (Fig. 2*b*), there was a marked decrease in NFκB binding activity compared with R2FDD cells (Fig. 2*c*), suggesting that p53 activation inhibited NFκB DNA binding activity after T-oligo treatment.

We then evaluated the effect of T-oligos on NFκB-driven transcription by transfecting R2FWT and R2FDD cells with an NFκB reporter plasmid. In cells expressing $p53^{WT}$, within 24 h T-oligo treatment decreased NFκB-driven transcription by ~35%, whereas in $p53^{DN}$ cells T-oligo treatment had no inhibitory effect on NFκB-driven transcription (Fig. 2*d*). We next transfected these cells with the COX-2 reporter plasmid. In R2FWT cells, treatment with T-oligos decreased COX-2 transcription by more than 50%, whereas in R2FDD cells T-oligo treatment had virtually no effect (Fig. 2*e*). In combination, these results demonstrate that functional p53 is required for T-oligo-induced repression of the COX-2 promoter and suggest that the effect may be mediated at least in part through NFκB.

To examine if T-oligo-induced p53-mediated repression of the COX-2 promoter depends on inhibition of NFκB transcriptional activity, we evaluated the effect of T-oligo treatment on NFκB-driven transcription by transfecting R2FWT and R2FDD cells with the COX-2 gene promoter with a site-specific mutation of the NFκB binding region (see diagram in Fig. S4*a*). In R2FWT cells transfected with WT COX-2 promoter, treatment with T-oligos decreased COX-2 transcription by more than 70%, whereas in R2FWT cells transfected with the mutated COX-2 promoter, T-oligo treatment had no inhibitory effect (Fig. S4*b*). In R2FDD cells, transfected with either WT or NFκB mutant COX-2 plasmid, T-oligo treatment had no effect (data not shown). These data demonstrate direct involvement of NFκB in T-oligo-induced p53-mediated repression of COX-2 promoter.

T-oligo Pretreatment Down-regulates Base-line and UVB-induced COX-2 Protein Levels in Human Keratinocytes, Coinciding with Activation of p53, p53-dependent Inhibition of NFκB Activity, and NFκB-dependent Transactivation—Because keratinocytes are a primary target for UVB damage and are the cells that give rise to UV light-induced actinic keratoses and SCC, we also examined the effect of T-oligos on primary human keratinocytes. Keratinocytes were pretreated with either T-oligos or diluent alone for 48 h and then sham or UV light-irradiated. Cells were then placed in medium without T-oligos and harvested for analysis of COX-2 protein levels and p53 DNA binding activity 8 and 24 h after irradiation. As shown by Western blot analysis (Fig. 3*a*) and quantified by densitometry (Fig. S5) in sham-irradiated keratinocytes, constitutive COX-2 expression was low at 8 and 24 h and similar in diluent-treated *versus* T-oligo-treated cells.

As reported previously (27, 74), UV irradiation markedly up-regulated COX-2 within 24 h in diluent-treated control cells (Fig. 3*b* and Fig. S5). However, as expected if T-oligos negatively regulate COX-2 in keratinocytes as well as in fibroblasts, COX-2 levels in T-oligo-treated keratinocytes were reduced by >50% at both 8 and 24 h (Fig. 3*b* and Fig. S5), the time of maximal UV light-induced COX-2 protein expression reported by others in this cell type (27, 74).

To substantiate further the involvement of p53 in T-oligo-induced down-regulation of COX-2 expression in human keratinocytes, we next evaluated T-oligo-mediated changes in p53 DNA binding activity using the protein from the same samples that was used to evaluate COX-2 protein levels in keratinocytes. At 8 and 24 h, EMSA showed minimal p53 DNA binding activity in T-oligo-treated or diluent-treated sham-irradiated cells, similar to the negative control (Fig. 3*c*, *lanes 7–10 versus 2*). As expected, UV irradiation increased p53 binding activity in dilu-

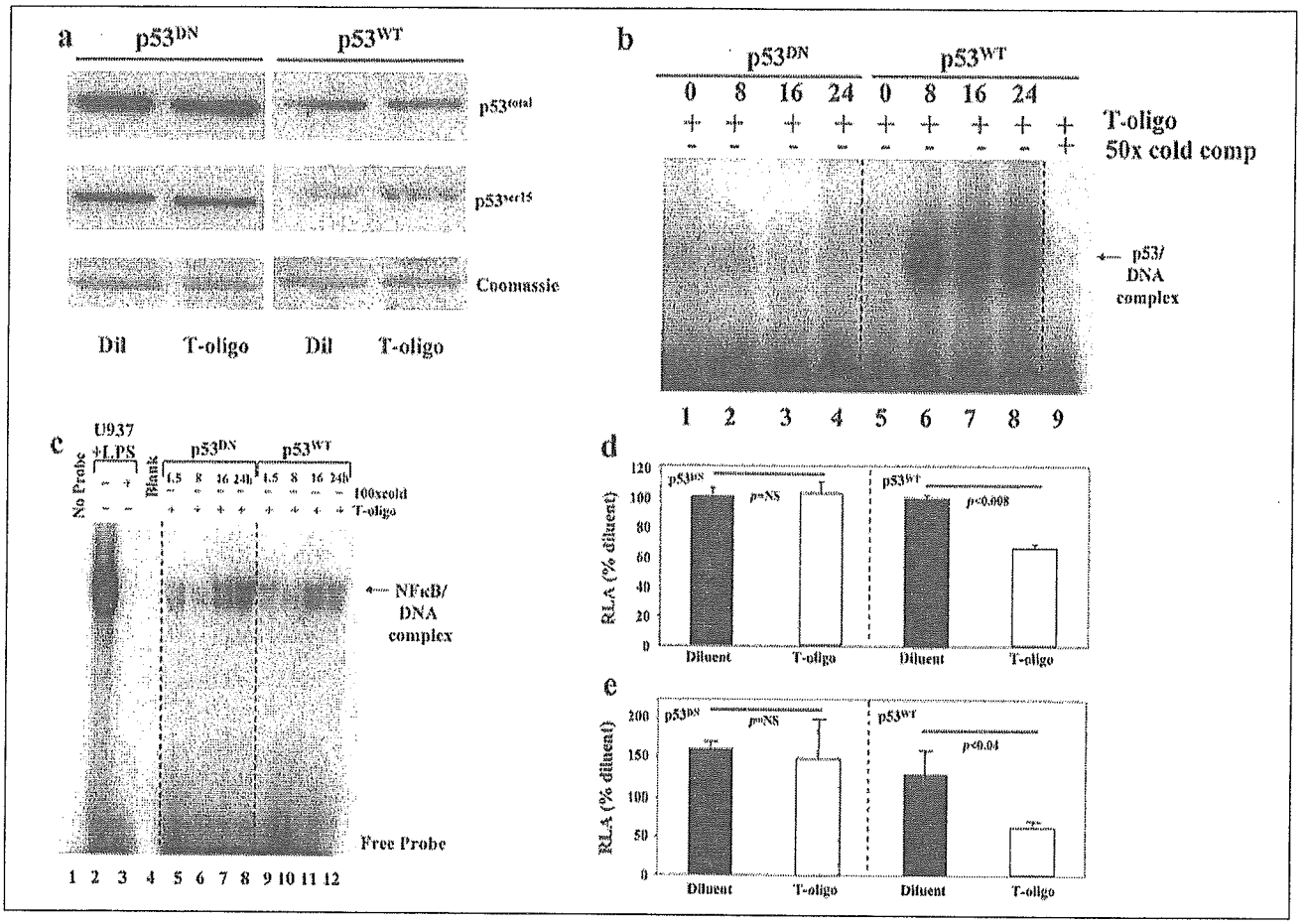

FIGURE 2. **T-oligo down-regulates COX-2 promoter activity through activation of p53.** R2FWT and R2FDD were additionally transiently transfected with a full-length COX-2 promoter-firefly luciferase reporter construct. *a*, cells treated once 48 h after transfection with either diluent or T-oligo (p9-mer 40 μM) and then processed for Western blot analysis after 24 h. In R2WT cells, T-oligo increased $p53^{Ser15}$ levels and minimally increased $p53^{total}$ levels compared with diluent treatment. However, in R2FDD cells, there was a high base-line expression of $p53^{total}$ and $p53^{Ser15}$ with no up-regulation by T-oligo. *b*, nuclear protein isolated from paired cultures 8, 16, and 24 h after addition of T-oligo (p9-mer 40 μM) shows substantial p53 DNA binding activity only in R2FWT cells. Specificity of binding is confirmed by the disappearance of the band in the control lane of R2FWT cell lysate treated with T-oligos for 24 h, reacted with a 50× excess of cold probe. *c*, nuclear protein isolated from paired cultures after T-oligo (p9-mer 40 μM) addition in fresh medium showed a bi-phasic pattern of NFκB DNA binding activity in R2FDD as well as R2FWT cells, but at 24 h, the time of increased p53 activity in R2FWT cells, NFκB binding activity was markedly decreased. Specificity of binding is confirmed by lack of a band in the *control lane 3* reacted with a 100× excess of cold probe compared with the strong positive band in *lane 2* containing a nuclear extract of lipopolysaccharide (*LPS*)-treated U937 cells. *d*, all cells were co-transfected with a *Renilla* luciferase reporter, to normalize for transfection efficiency of the NFκB reporter plasmid or the empty vector pGL2, a negative control. Transfectants were treated once with either diluent or T-oligo for 24 h before harvesting for the dual luciferase assay. A set of cells was transfected with the empty vector used to create the NFκB reporter construct. Results shown are the average of three separate experiments in duplicate for relative luciferase activity (*RLA*) for the firefly *versus Renilla* luciferase in the same dishes. In R2FWT cells, T-oligo treatment (p9-mer 40 μM) decreased NFκB-driven transcription by ~34% (100 ± 3 *versus* 66 ± 4, $p < 0.008$, diluent *versus* T-oligo), but in R2FDD cells, treatment with T-oligo had no effect (100 ± 11 *versus* 102 ± 16, $p = 0.8$, diluent *versus* T-oligo). *e*, all cells were processed as described in *d* but were transfected with a COX-2 promoter construct. Results shown are the average of three separate experiments in triplicate with firefly luciferase values normalized against *Renilla* luciferase values in the same dishes. In R2FWT cells, T-oligo treatment (p9-mer 40 μM) decreased COX-2 promoter activity by ~50% (125 ± 30 *versus* 58 ± 8, $p < 0.04$, diluent *versus* T-oligo), but in the R2FDD cells, T-oligo treatment had no effect (100 ± 6 *versus* 94 ± 30, p = not significant (*NS*), diluent *versus* T-oligo).

ent-treated keratinocytes between 8 and 24 h (Fig. 3*c*, *lanes 3 versus 5*). However, in T-oligo-treated UV light-irradiated keratinocytes, p53 binding activity was increased 4-fold as early as 8 h after UVB compared with the levels in diluent-treated UV light-irradiated cells (Fig. 3*c*, *lanes 4 versus 3*), although by 24 h p53 DNA binding activity was less and was comparable in diluent- *versus* T-oligo-treated UV light-irradiated samples (Fig. 3*c*, *lanes 6 versus 5*). These data confirm an inverse relationship between p53 activity and COX-2 levels in human keratinocytes, as well as in fibroblasts.

Because NFκB is a known positive regulator of COX-2 transcription and we found that T-oligo treatment inhibits NFκB DNA binding activity in fibroblasts, experiments were performed to confirm this presumptive mechanism for indirect T-oligo-mediated p53-dependent inhibition of COX-2 transcription in keratinocytes. We reasoned that a possible limiting factor for the transcriptional activity of both p53 and NFκB may be the binding to the transcriptional co-activator protein p300 (70, 75). To address this possibility, we pretreated human keratinocytes with diluent or T-oligo for 24 h. Cells were then UV light-irradiated with 15 mJ/cm^2 followed by incubation in medium without T-oligos for 8 and 24 h and harvested for immunoprecipitation with anti-p300 antibodies followed by Western blot analysis for NFκB/p65 and p53 (Fig. 3*d*). In diluent-treated UV light-irradiated keratinocytes, NFκB/p65 binding to p300 increased markedly between 8 and 24 h after UV irradiation (Fig. 3*d*, *lanes 1 versus 3*). In contrast, in T-oligo-pretreated UV light-irradiated keratinocytes, NFκB binding to p300 was decreased relative to control as early as 8 h, and by 24 h NFκB binding to p300 was virtually undetectable (Fig. 3*d lanes 2 versus 4*). These data strongly suggest that T-oligo treatment decreases NFκB transcriptional activity via reduction of NFκB binding to its transcriptional co-activator p300 protein. Consistent with this interpretation, the amount of p53 binding to p300 was strikingly increased in T-oligo-treated *versus* control cells at both 8 and 24 h (Fig. 3*d*, *lanes 1* and *3 versus 2* and *4*, respectively). These data are consistent with an indirect mechanism of T-oligo-mediated p53-dependent inhibition of NFκB transcriptional

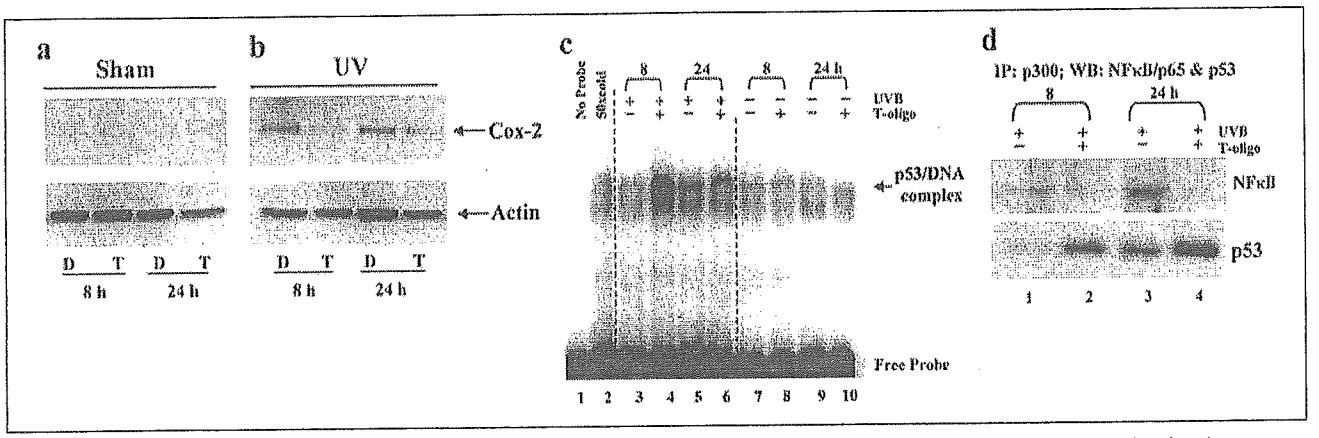

FIGURE 3. **T-oligo pretreatment activates p53 and down-regulates constitutive and UV light-induced COX-2 expression in keratinocytes.** Human newborn keratinocytes were treated as in Fig. 1. *a*, paired dishes were then sham-irradiated and harvested after 8 and 24 h for evaluation of COX-2 and actin (loading control) protein levels. These experiments were repeated two times with similar results. *b*, paired dishes were then UVB-irradiated with 15 mJ/cm^2, harvested, and processed as for *a*. At 8 h COX-2 expression was comparable in diluent-treated and T-oligo-treated samples. In UV light-irradiated control samples, COX-2 expression increased by 8 h with a further increase at 24 h, whereas in T-oligo-treated UV light-irradiated cells, COX-2 expression was significantly down-regulated throughout the 24 h. Similar results were obtained in three independent experiments. *c*, cells lysates from the same samples that were used to evaluate COX-2 protein levels in keratinocytes in *a* were used to evaluate T-oligo-mediated changes in p53 DNA binding activity in EMSA. Specificity of binding is confirmed by significant reduction of the band in the control lane using 50× excess of cold probe and protein lysate of keratinocytes treated with T-oligos for 8 h (*lane 2 versus lane 4*). *d*, cell lysates from the same samples that were used to evaluate COX-2 protein levels and p53 binding activity in keratinocytes in *b* and *c* (only T-oligo-treated UV light-irradiated) were used for immunoprecipitation (*IP*) with anti-p300 antibodies followed by Western blot analysis for NFκB/p65 and p53. T-oligo treatment decreased binding of NFκB to p300 by 8 h and was virtually undetectable by 24 h, whereas in T-oligo-treated UB-irradiated keratinocytes p53 binding to p300 was increased already by 8 h and was even greater by 24 h.

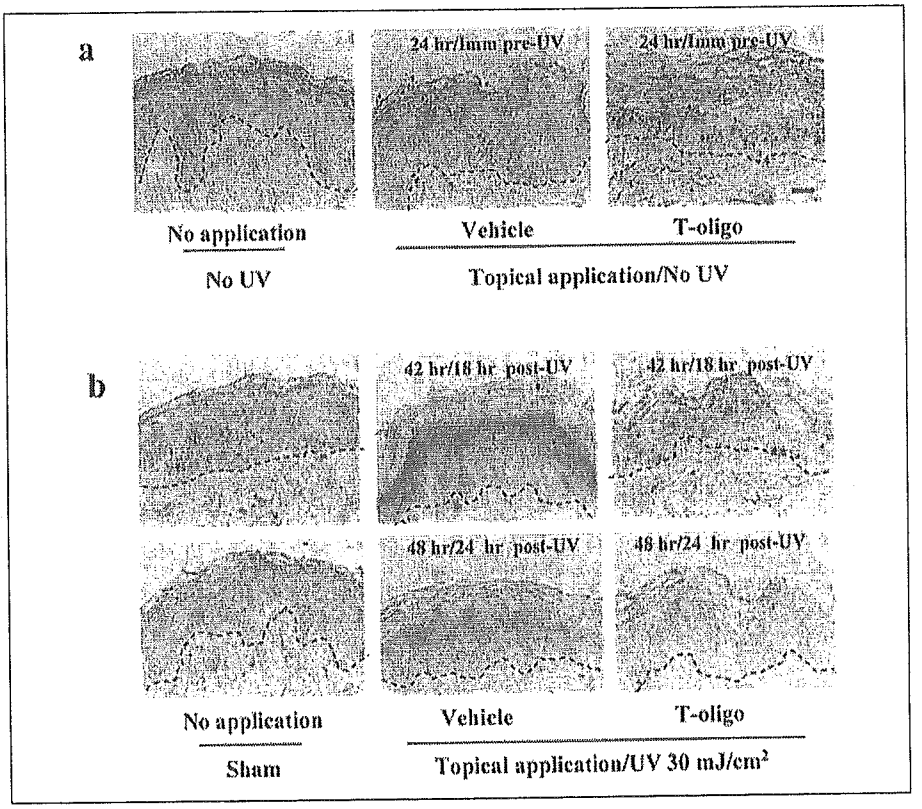

FIGURE 4. **T-oligo treatment decreases constitutive and UVB-induced COX-2 levels in human skin explants.** Human skin explants (10 per donor, 5 for each T-oligo) were prepared from otherwise discarded normal adult skin and treated immediately as described under "Experimental Procedures." Untreated nonirradiated skin showed constant low COX-2 expression over the 48-h experiment. *a*, in paired explants harvested after 24 h, T-oligos (pTT 100 μM; p9-mer data not shown) modestly decreased low base-line levels of COX-2 expression in the suprabasal epidermis. *b*, in paired explants harvested after T-oligo treatment and subsequent UVB irradiation, T-oligos strikingly decreased UVB-induced levels of COX-2 expression in the suprabasal epidermis as early as 18 h and continued through 24 h after irradiation. Specificity of COX-2 antibody staining was confirmed by staining sections of nontreated and diluent/T-oligo-treated and UVB-irradiated samples with mixed keratin human monoclonal mouse anti-human antibodies (DakoCytomation, Carpinteria, CA). No difference in epidermal staining pattern between nontreated and treated and then UV light-irradiated samples was detected, suggesting specificity of COX-2 antibody staining (Fig. S6, *a* and *b*). Dermal epidermal junction is indicated by the *dashed line*; ×200 magnification, all panels.

activity in which activated p53 successfully competes with NFκB for binding to their common co-activator, p300.

T-oligo Pretreatment Down-regulates Both Base-line and UVB-induced COX-2 Expression in Human Explants—The effect of T-oligos on COX-2 levels in human skin was studied using adult skin explants. Explants were treated as described under "Experimental Procedures" and then processed for immunostaining for COX-2, p53^{total}, and phospho-p53^{Ser15} levels. COX-2 was constitutively expressed throughout the epidermis, particularly in the suprabasal layers, as reported previously (76). Pretreatment with T-oligos modestly down-regulated constitutive COX-2 levels (Fig. 4*a*) and strongly inhibited UV light-induced COX-2 levels (Fig. 4*b*). By 18 and 24 h after a single 30 mJ/cm^2 dose of UVB, there was a significant decrease in COX-2 immunostaining in T-oligo-treated skin treated once 42 or 48 h previously with T-oligo when compared with sham-irradiated untreated control skin. In contrast, in vehicle-treated skin there was a dramatic

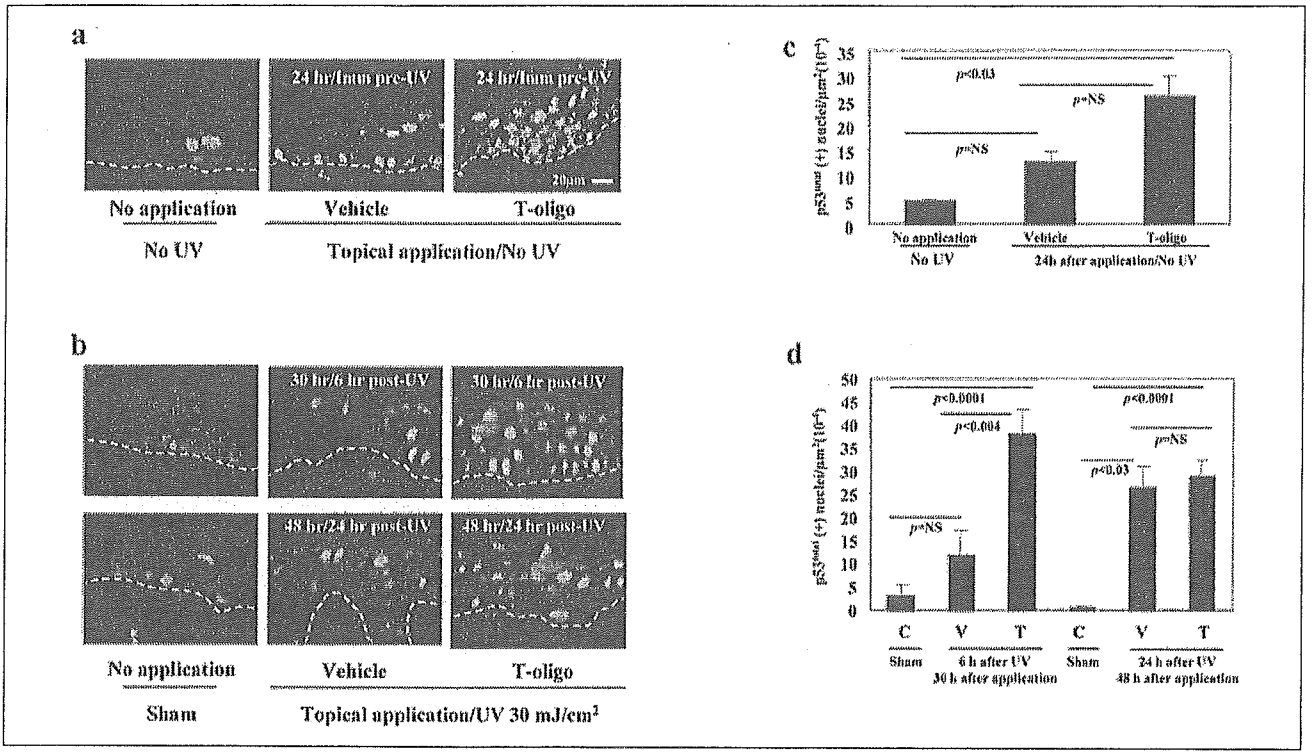

FIGURE 5. **T-oligo treatment increases constitutive and UVB-induced $p53^{total}$ levels in human skin.** Adjacent sections of the same explants shown in Fig. 4 were reacted with a fluorescently tagged antibody to total p53 and examined under a fluorescent microscope. There is no change in low p53 expression in untreated nonirradiated explants over the 48-h experiment. *a*, T-oligo (pTT 100 μM; p9-mer data not shown) increased constitutive levels of $p53^{total}$ expression, as shown by the number of positive (+) nuclei in the epidermis. *b*, T-oligo treatment increases UV light-induced $p53^{total}$ expression 6 h after UVB, but the number of (+) nuclei in T-oligo *versus* vehicle-treated explants is comparable after 24 h and far greater than in sham-irradiated control explants. *c* and *d*, quantitative analysis of $p53^{total}$ (+) nuclei as determined by blindly examining at least 3–5 fields (×200) and averaging. Values are expressed per 10^{-4} μm^2 of epidermal area and represent explants prepared from three donors. In addition, to confirm the validity of quantifying $p53^{total}$ (+) nuclei per 10^{-4} μm^2 of epidermal area, we also quantified $p53^{total}$ (+) nuclei per number of nuclei (4′,6-diamidino-2-phenylindole + cells). No difference in the relative expression of $p53^{total}$ (+) nuclei was found using either quantification method (Fig. S7, *a* and *b*). Note that after 24 h nonirradiated T-oligo-treated explants have p53 positivity comparable with that of UV light-irradiated explants. *C*, control; *V*, vehicle; *T*, T-oligo; *NS*, not significant. ×200 magnification in all panels.

increase in COX-2 immunostaining by 16 h that diminished slightly but persisted through 24 h (Fig. 4*b*).

T-oligo-induced Inhibition of COX-2 Expression in Human Skin Is Associated with Up-regulation and Activation of p53 Protein—To confirm our *in vitro* findings of an inverse relationship between T-oligo-induced decreases in constitutive and UV light-induced COX-2 levels and increases in p53 level and activity, adjacent sections of the same human tissue that were used for COX-2 immunostaining were processed for both $p53^{total}$ and $p53^{Ser15}$ immunofluorescent staining. In T-oligo-treated *versus* vehicle-treated skin after 24 h, there was a >100% increase in the number of constitutively $p53^{total}$ positive (+) nuclei (26 ± 4 *versus* 12 ± 2, $p < 0.09$) (Fig. 5, *a* and *c*). In UV light-irradiated samples by 6 h the numbers of $p53^{total}$ (+) nuclei in T-oligo-treated samples were increased more than 3-fold above vehicle controls (38 ± 5 *versus* 12 ± 6, $p < 0.004$), and more than 10-fold above sham-irradiated samples, whereas the modest and variable increase in UV light-irradiated control samples remained insignificant (Fig. 5, *b* and *d*). By 24 h, the numbers of $p53^{total}$ (+) nuclei were similar in T-oligo-*versus* diluent-treated UV light-irradiated skin samples (29 ± 4 *versus* 26 ± 5, $p = 0.6$) and more than 20-fold higher in both cases than in the sham-irradiated controls (Fig. 5, *b* and *d*).

T-oligo treatment minimally increased the number of nuclei with detectable constitutive $p53^{Ser15}$ levels (0.3 ± 0.2 *versus* 0.5 ± 0.2, vehicle *versus* T-oligo, $p = 0.09$) (Fig. 6, *a* and *c*). However, compared with vehicle-treated UV light-irradiated skin, there was a modest but statistically significant increase in the number of $p53^{Ser15}$ (+) nuclei in T-oligo-treated UV light-irradiated skin samples at 6 and 24 h (6 h, 10.3 ± 0.8 *versus* 14 ± 0.6, $p < 0.001$; and 24 h, 8.5 ± 0.9 *versus* 13 ± 0.6, vehicle *versus* T-oligo, $p < 0.001$) as well as striking and highly significant increases above sham-irradiated untreated samples in both cases (Fig. 5, *b* and *d*). Taken together with the data of COX-2 immunostaining (Fig. 4*b*), these results establish an *in vivo* relevance of the cause-and-effect inverse relationship between increased p53 levels and activity and decreased COX-2 levels in T-oligo-treated human fibroblasts and keratinocytes (Fig. 1, *a* and *b*, and Fig. 3, *a–c*).

368

DISCUSSION

UV irradiation is the major environmental carcinogen for human skin (77, 78), initiating and promoting development of both melanoma and nonmelanoma skin cancers (79–81). Mechanisms that contribute to UV light-induced mutagenesis and carcinogenesis include inactivation of tumor suppressor genes and/or activation of oncogenes (82–84), events that may also lead to clonal expansion of affected cells (85–89). However, in recent years a great deal of evidence has emerged suggesting that UV light-induced inflammation also plays an important role in tumor promotion and progression (26, 90–93). In murine models of skin carcinogenesis, it has been shown that administration of nonsteroidal anti-inflammatory drugs, especially selective COX-2 inhibitors, reduces the prevalence and multiplicity of UV light-induced neoplasms (74, 92–95), strongly implying direct involvement of COX-2 in cutaneous carcinogenesis.

The present study demonstrates that topical application of telomere 3′-overhang homolog DNA oligonucleotides, collectively termed T-oligos, inhibits UV light-induced up-regulation of COX-2 *in vitro* and *ex*

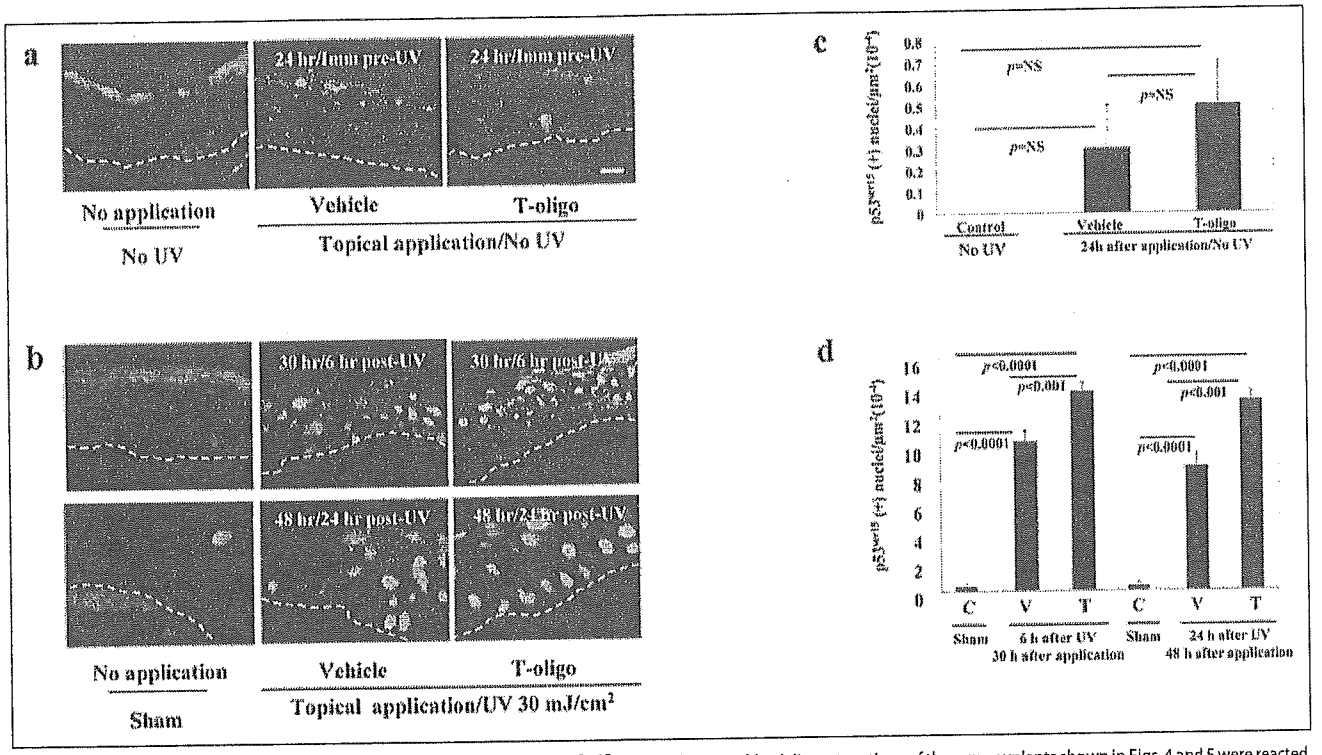

FIGURE 6. **T-oligos treatment increases constitutive and UVB-induced $p53^{Ser15}$ levels in human skin.** Adjacent sections of the same explants shown in Figs. 4 and 5 were reacted with a fluorescently tagged antibody to phospho-$p53^{Ser15}$ and then analyzed as described for Fig. 5. T-oligo (pTT 100 μM; p9-mer data not shown) treatment variably and minimally increased constitutive levels of $p53^{Ser15}$ expression (*a*) with the number of $p53^{Ser15}$ (+) nuclei in the epidermis consistently below 0.7 per $\mu m^2 \times 10^{-4}$ in all groups (p = not significant (*NS*)). *c*, nonspecific retention of label in the stratum corneum was also observed in most specimens. After UV irradiation, the number of $p53^{Ser15}$ (+) nuclei increased dramatically compared with sham-irradiated controls within 6 h and through 24 h for both T-oligo- and vehicle-treated explants. *b*, quantitative analysis of $p53^{Ser15}$ (+) nuclei performed as for Fig. 5 revealed a roughly 20–30-fold increase in $p53^{Ser15}$ above preirradiation levels for both vehicle-treated and T-oligo-treated explants, with T-oligo-treated explants showing ~40 and 53% higher numbers of (+) nuclei at 6 and 24 h, respectively, a significant difference ($p < 0.001$) at both times (*d*). ×200 magnification, *a* and *b*, *upper panel*; ×400 magnification, *b*, *lower panel*.

vivo in human skin. These data expand our earlier reports that T-oligos elicit UV light-protective and cancer-preventative responses in skin cells (40, 45, 46, 50, 51). Most if not all of these responses are mediated at least in part through up-regulation and activation of p53, with subsequent effects on p53-regulated downstream target genes (49–51, 55, 56). Our current data show that T-oligo-dependent UV light-protective responses can be mediated specifically by transcriptional repression of gene products such as the inducible isoform of cyclooxygenase, COX-2 (17), that catalyzes the rate-limiting step of prostaglandin and thromboxane production (18–20). Western blot analysis of normal human fibroblasts and keratinocytes showed an inverse relationship between p53 up-regulation and activation and down-regulation of constitutive and UV light-induced COX-2 levels in both cell types. Studies in paired isogenic fibroblast lines with wild type *versus* dominant negative p53 confirmed that p53 transcriptional activity is required for this effect on COX-2. In addition, the present study also demonstrates that T-oligo addition to human skin explants up-regulates and activates constitutive p53 and, after subsequent UV light exposure, blocks COX-2 overexpression.

We demonstrate that T-oligos decrease COX-2 levels at least in part by decreasing COX-2 transcription, an effect that is dependent on p53 activity, not on total p53 levels. It is known that p53 suppresses a variety of promoters that contain one or more TATA boxes (96, 97). It was suggested that p53 suppresses gene expression by interfering with formation of the transcription preinitiation complex with TATA-binding proteins (TBPs) by preventing binding of TBPs to the TATA motif (98). Many genes are reported to be negatively regulated by p53. These include c-*Fos*, c-*Jun*, c-*Myc*, *IL-6*, heat shock protein 70 gene (*HSP70*), multidrug resistance gene (*MDR1*), and B-cell lymphoma gene-2 (*Bcl2*) (98–103).

Relevant to p53-dependent regulation of COX-2, it was shown that p53 inhibits the formation of complexes between TBPs and the murine and human COX-2 promoters in a cell-free system (33). The same authors also reported that wild type but not temperature-sensitive mutant p53 competed with TATA-binding proteins for binding to the mouse and human COX-2 promoters over a 100-bp segment surrounding the transcription initiation start on COX-2 promoter (33). Accordingly, to test the hypothesis that T-oligo-mediated p53-dependent suppression of COX-2 depends on repression of COX-2 promoter activity by activated p53, we tested T-oligo effect in $p53^{WT}$ *versus* $p53^{DN}$ cells. In cells expressing $p53^{WT}$, treatment with T-oligos decreased constitutive COX-2 promoter-driven transcription of a reporter plasmid by 54%, whereas in $p53^{DN}$ cells T-oligo treatment had virtually no effect on COX-2 promoter activity, demonstrating that functional p53 is required for T-oligo-induced repression of the COX-2 promoter. Our findings may also resolve apparently conflicting data in the literature concerning regulation of *COX-2* gene expression by p53, as investigators reporting positive p53 regulation of COX-2 in various mutant and tumor-derived cell lines correlated only the level of expression of the two proteins and did not assess p53 activity (104).

Cellular responses to DNA-damaging stimuli, including UV irradiation, are usually complex and often regulated by more than one transcription factor, for example by both p53 and NFκB (105). Furthermore, several studies have established a reciprocal inhibitory regulation of the transcription factors NFκB and p53 in various cell lines treated with DNA-damaging agents, mediated through competitive binding of p53 and NFκB to the transcriptional co-activator p300 protein (69, 70, 106). We found that in human fibroblasts and keratinocytes, T-oligo treat-

ment up-regulates and activates p53, coinciding with decreased NFκB DNA binding activity and inhibition of transcription from NFκB-driven promoter constructs. Moreover, in human keratinocytes we also showed that treatment with T-oligo prior to UV irradiation inhibited p300 binding to NFκB and increased p300 binding to p53, as shown by immunoprecipitation of p300, followed by Western blot for NFκB/p65 and p53 proteins, coinciding with p53 activation and decreased COX-2 expression. This second and indirect mechanism of inhibition of COX-2 expression may explain the somewhat delayed T-oligo-mediated inhibition of COX-2 expression observed in our studies. Alternatively or in addition, the detailed regulation of COX-2 may also depend on the stimulus, cell type, and tissue environment, leading to predominant/selective regulation of the COX-2 promoter at different times by such known positive transcription factors as AP1, NF-IL6, NFκB, NFAT, and PEA3 (19). In fact, in our previous publications we have shown that T-oligos appear to exert their protective effects by activating ATM kinase (38) and its downstream effectors, including p53 and p95/Nbs1 (38, 40, 49), as well as by up-regulating a variety of other genes including *E2F1*, $p16^{INK4a}$, and the *p53* homologue *p73* not known to be regulated by ATM (38–40, 49, 55).

E2F1 may be of particular relevance to our findings, as there is evidence suggesting E2F1 mediated inhibition of NFκB in various cell types (107, 108). Indeed, Tanaka *et al.* (107) showed that endogenous E2F1 competes with NFκB/p50 for binding to the p65 subunit of NFκB and that this physical interaction of E2F1/p65 inhibits NFκB transcriptional activities. Additionally, Phillips *et al.* (109) have shown in Saos2 cells lacking p53 that E2F1-induced inhibition of NFκB nuclear translocation and activity is mediated by the abrogation of TRAF-2 protein and inhibition of IκB kinase phosphorylation. It will be of interest to further investigate, specifically in cells with nonfunctional p53, such as the majority of UV light-induced skin neoplasms, whether T-oligo-mediated E2F1-dependent inhibition of NFκB in the absence of functional p53 may also inhibit COX-2 expression.

To date, attention has been directed toward inhibition of COX-2 enzyme activity, and much less attention has been given to modulation of COX-2 protein levels that are constitutively increased in many tumor cells (110). However, compared with young skin, there is an age-associated increase in constitutive and UV light-induced prostaglandin E_2 production and COX-2 expression in human skin (26). The resulting chronic low grade inflammation may have crucial pathophysiologic implications for many aging processes, such as loss of collagen, and may contribute to the development and progression of age-associated diseases, including malignancies. Indeed, experimental COX-2 overexpression has been also reported to increase tumorigenesis in a variety of organ systems, including colon, lung, prostate, breast cancer, urinary bladder, pancreas, and liver (76, 111–115), in addition to skin (26–29). COX-2 overexpression is also increasingly implicated in the process of tumor angiogenesis (neovascularization) through increasing vascular endothelial growth factor levels as well as producing prostaglandins and thromboxanes that promote endothelial cell migration (18).

We conclude that T-oligo treatment beneficially affects multiple contributors to carcinogenesis; T-oligos transiently inhibit cell proliferation (38–41, 44–51, 55, 56), enhance DNA repair capacity (49–51), and decrease mutagenesis and photocarcinogenesis (51), as well as induce apoptosis and senescence of malignant cells (38, 40, 42, 43). In the present report we demonstrate that T-oligos also decrease constitutive and UV light-induced levels of COX-2, an inflammatory mediator strongly implicated in the processes of photocarcinogenesis, chemical and spontaneous carcinogenesis, and tumor angiogenesis (116–118). Furthermore, we suggest that T-oligos may also combat the tendency for chronic low grade inflammation that accompanies aging (26).

Acknowledgments—We are grateful to Dr. Christina Wu and Cynthia Curry for their valuable assistance in promoter regulation studies and to Kathleen Huard and Daniella Adrien for assistance in preparation of the manuscript.

REFERENCES

1. Jemal, A., Murray, T., Ward, E., Samuels, A., Tiwari, R. C., Ghafoor, A., Feuer, E. J., and Thun, M. J. (2005) *CA–Cancer J. Clin.* **55**, 10–30
2. Albert, M. R., and Weinstock, M. A. (2003) *CA–Cancer J. Clin.* **53**, 292–302
3. Geller, A. C., Zhang, Z., Sober, A. J., Halpern, A. C., Weinstock, M. A., Daniels, S., Miller, D. R., Demierre, M. F., Brooks, D. R., and Gilchrest, B. A. (2003) *J. Am. Acad. Dermatol.* **48**, 34–41
4. Brash, D. E., and Ponten, J. (1998) *Cancer Surv.* **32**, 69–113
5. Zoumpourlis, V., Solakidi, S., Papathoma, A., and Papaevangeliou, D. (2003) *Carcinogenesis* **24**, 1159–1165
6. Patrick, M. H. (1977) *Photochem. Photobiol.* **25**, 357–372
7. Wood, R. D. (1996) *Annu. Rev. Biochem.* **65**, 135–167
8. de Gruijl, F. R., van Kranen, H. J., and Mullenders, L. H. (2001) *J. Photochem. Photobiol. B Biol.* **63**, 19–27
9. Sterenborg, H. J., de Gruijl, F. R., and van der Leun, J. C. (1986) *Photodermatol.* **3**, 206–214
10. Lavker, R. M., Gerberick, G. F., Veres, D., Irwin, C. J., and Kaidbey, K. H. (1995) *J. Am. Acad. Dermatol.* **32**, 53–62
11. Remenyik, E., Wikonkal, N. M., Zhang, W., Paliwal, V., and Brash, D. E. (2003) *Oncogene* **22**, 6369–6376
12. Aubin, F. (2003) *Eur. J. Dermatol.* **13**, 515–523
13. Schwarz, T. (2002) *Photodermatol. Photoimmunol. Photomed.* **18**, 141–145
14. Bielenberg, D. R., Bucana, C. D., Sanchez, R., Donawho, C. K., Kripke, M. L., and Fidler, I. J. (1998) *J. Invest. Dermatol.* **111**, 864–872
15. Hruza, L. L., and Pentland, A. P. (1993) *J. Invest. Dermatol.* **100**, 35S–41S
16. Furstenberger, G., Gross, M., and Marks, F. (1989) *Carcinogenesis* **10**, 91–96
17. Brecher, A. R. (2002) *J. Drugs Dermatol.* **1**, 44–47
18. Turini, M. E., and DuBois, R. N. (2002) *Annu. Rev. Med.* **53**, 35–57
19. Dannenberg, A. J., and Subbaramaiah, K. (2003) *Cancer Cell* **4**, 431–436
20. Parente, L., and Perretti, M. (2003) *Biochem. Pharmacol.* **65**, 153–159
21. Howe, L. R., Subbaramaiah, K., Brown, A. M., and Dannenberg, A. J. (2001) *Endocr. Relat. Cancer* **8**, 97–114
22. Castelao, J. E., Bart, R. D., 3rd, DiPerna, C. A., Sievers, E. M., and Bremner, R. M. (2003) *Ann. Thorac. Surg.* **76**, 1327–1335
23. Marnett, L. J., and DuBois, R. N. (2002) *Annu. Rev. Pharmacol. Toxicol.* **42**, 55–80
24. Ferrandez, A., Prescott, S., and Burt, R. W. (2003) *Curr. Pharm. Des.* **9**, 2229–2251
25. Chen, W., Tang, Q., Gonzales, M. S., and Bowden, G. T. (2001) *Oncogene* **20**, 3921–3926
26. Seo, J. Y., Kim, E. K., Lee, S. H., Park, K. C., Kim, K. H., Eun, H. C., and Chung, J. H. (2003) *Mech. Ageing Dev.* **124**, 903–910
27. An, K. P., Athar, M., Tang, X., Katiyar, S. K., Russo, J., Beech, J., Aszterbaum, M., Kopelovich, L., Epstein, E. H., Jr., Mukhtar, H., and Bickers, D. R. (2002) *J. Photochem. Photobiol. B Biol.* **76**, 73–80
28. Orengo, I. F., Gerguis, J., Phillips, R., Guevara, A., Lewis, A. T., and Black, H. S. (2002) *Arch. Dermatol.* **138**, 751–755
29. Fischer, S. M., Conti, C. J., Viner, J., Aldaz, C. M., and Lubet, R. A. (2003) *Carcinogenesis* **24**, 945–952
30. Muller-Decker, K., Neufang, G., Berger, I., Neumann, M., Marks, F., and Furstenberger, G. (2002) *Proc. Natl. Acad. Sci. U. S. A.* **99**, 12483–12488
31. Ahmed, S., Rahman, A., Hasnain, A., Lalonde, M., Goldberg, V. M., and Haqqi, T. M. (2002) *Free Radic. Biol. Med.* **33**, 1097–1105
32. Ospina, J. A., Brevig, H. N., Krause, D. N., and Duckles, S. P. (2004) *Am. J. Physiol.* **286**, H2010–H2019
33. Subbaramaiah, K., Altorki, N., Chung, W. J., Mestre, J. R., Sampat, A., and Dannenberg, A. J. (1999) *J. Biol. Chem.* **274**, 10911–10915
34. Gallo, O., Schiavone, N., Papucci, L., Sardi, I., Magnelli, L., Franchi, A., Masini, E., and Capaccioli, S. (2003) *Am. J. Pathol.* **163**, 723–732
35. Griffith, J. D., Comeau, L., Rosenfield, S., Stansel, R. M., Bianchi, A., Moss, H., and de Lange, T. (1999) *Cell* **97**, 503–514
36. Stansel, R. M., de Lange, T., and Griffith, J. D. (2001) *EMBO J.* **20**, 5532–5540
37. Karlseder, J., Broccoli, D., Dai, Y., Hardy, S., and de Lange, T. (1999) *Science* **283**, 1321–1325
38. Eller, M. S., Li, G. Z., Firoozabadi, R., Puri, N., and Gilchrest, B. A. (2003) *FASEB J.* **17**, 152–162
39. Li, G. Z., Eller, M. S., Firoozabadi, R., and Gilchrest, B. A. (2003) *Proc. Natl. Acad. Sci. U. S. A.* **100**, 527–531
40. Eller, M. S., Puri, N., Hadshiew, I. M., Venna, S. S., and Gilchrest, B. A. (2002) *Exp.*

Cell Res. **276**, 185–193
41. Hadshiew, I. M., Eller, M. S., Gasparro, F. P., and Gilchrest, B. A. (2001) *J. Dermatol. Sci.* **25**, 127–138
42. Puri, N., Eller, M. S., Byers, H. R., Dykstra, S., Kubera, J., and Gilchrest, B. A. (2004) *FASEB J.* **18**, 1373–1381
43. Li, G. Z., Eller, M. S., Hanna, K., and Gilchrest, B. A. (2004) *Exp. Cell Res.* **301**, 189–200
44. Pedeux, R., Al-Irani, N., Marteau, C., Pellicier, F., Branche, R., Ozturk, M., Ranchi, J., and Dore, J. F. (1998) *J. Invest. Dermatol.* **111**, 472–477
45. Eller, M. S., Yaar, M., and Gilchrest, B. A. (1994) *Nature* **372**, 413–414
46. Eller, M. S., Ostrom, K., and Gilchrest, B. A. (1996) *Proc. Natl. Acad. Sci. U. S. A.* **93**, 1087–1092
47. Curiel-Lewandrowski, C., Venna, S. S., Eller, M. S., Cruikshank, W., Dougherty, I., Cruz, P. D., and Gilchrest, B. A. (2003) *Exp. Dermatol.* **12**, 145–152
48. Cruz, P. D., Jr., Leverkus, M., Dougherty, I., Gleason, M. J., Eller, M., Yaar, M., and Gilchrest, B. A. (2000) *J. Invest. Dermatol.* **114**, 253–258
49. Eller, M. S., Maeda, T., Magnoni, C., Atwal, D., and Gilchrest, B. A. (1997) *Proc. Natl. Acad. Sci. U. S. A.* **94**, 12627–12632
50. Goukassian, D. A., Bagheri, S., el-Keeb, L., Eller, M. S., and Gilchrest, B. A. (2002) *FASEB J.* **16**, 754–756
51. Goukassian, D. A., Helms, E., van Steeg, H., van Oostrom, C., Bhawan, J., and Gilchrest, B. A. (2004) *Proc. Natl. Acad. Sci. U. S. A.* **101**, 3933–3938
52. Tubo, R. A., and Rheinwald, J. G. (1987) *Oncogene Res.* **1**, 407–421
53. Shaulian, E., Zauberman, A., Ginsberg, D., and Oren, M. (1992) *Mol. Cell. Biol.* **12**, 5581–5592
54. Rheinwald, J. G., Hahn, W. C., Ramsey, M. R., Wu, J. Y., Guo, Z., Tsao, H., De Luca, M., Catricala, C., and O'Toole, K. M. (2002) *Mol. Cell. Biol.* **22**, 5157–5172
55. Goukassian, D. A., Eller, M. S., Yaar, M., and Gilchrest, B. A. (1999) *J. Invest. Dermatol.* **112**, 25–31
56. Maeda, T., Eller, M. S., Hedayati, M., Grossman, L., and Gilchrest, B. A. (1999) *Mutat. Res.* **433**, 137–145
57. Gilchrest, B. A., Zhai, S., Eller, M. S., Yarosh, D. B., and Yaar, M. (1993) *J. Invest. Dermatol.* **101**, 666–672
58. Werninghaus, K., Handjani, R. M., and Gilchrest, B. A. (1991) *Photodermatol. Photomed.* **8**, 236–242
59. Kishore, R., Spyridopoulos, I., Luedemann, C., and Losordo, D. W. (2002) *Circ. Res.* **91**, 307–314
60. Inoue, H., Yokoyama, C., Hara, S., Tone, Y., and Tanabe, T. (1995) *J. Biol. Chem.* **270**, 24965–24971
61. Inoue, H., Taba, Y., Miwa, Y., Yokota, C., Miyagi, M., and Sasaguri, T. (2002) *Arterioscler. Thromb. Vasc. Biol.* **22**, 1415–1420
62. Kishore, R., Luedemann, C., Bord, E., Goukassian, D., and Losordo, D. W. (2003) *Circ. Res.* **93**, 932–940
63. Athar, M., An, K. P., Morel, K. D., Kim, A. L., Aszterbaum, M., Longley, J., Epstein, E. H., Jr., and Bickers, D. R. (2001) *Biochem. Biophys. Res. Commun.* **280**, 1042–1047
64. Hall, P. A., McKee, P. H., Menage, H. D., Dover, R., and Lane, D. P. (1993) *Oncogene* **8**, 203–207
65. Ramsay, R. G., Ciznadija, D., Vanevski, M., and Mantamadiotis, T. (2003) *Int. J. Immunopathol. Pharmacol.* **16**, 59–67
66. Perfettini, J. L., Roumier, T., Castedo, M., Larochette, N., Boya, P., Raynal, B., Lazar, V., Ciccosanti, F., Nardacci, R., Penninger, J., Piacentini, M., and Kroemer, G. (2004) *J. Exp. Med.* **199**, 629–640
67. Margulies, L., and Sehgal, P. B. (1993) *J. Biol. Chem.* **268**, 15096–15100
68. Hung, J. H., Su, I. J., Lei, H. Y., Wang, H. C., Lin, W. C., Chang, W. T., Huang, W., Chang, W. C., Chang, Y. S., Chen, C. C., and Lai, M. D. (2004) *J. Biol. Chem.* **279**, 46384–46392
69. Webster, G. A., and Perkins, N. D. (1999) *Mol. Cell. Biol.* **19**, 3485–3495
70. Culmsee, C., Siewe, J., Junker, V., Retiounskaia, M., Schwarz, S., Camandola, S., El-Metainy, S., Behnke, H., Mattson, M. P., and Krieglstein, J. (2003) *J. Neurosci.* **23**, 8586–8595
71. Rodel, F., Hantschel, M., Hildebrandt, G., Schultze-Mosgau, S., Rodel, C., Herrmann, M., Sauer, R., and Voll, R. E. (2004) *Int. J. Radiat. Biol.* **80**, 115–123
72. Han, S. J., Ko, H. M., Choi, J. H., Seo, K. H., Lee, H. S., Choi, E. K., Choi, I. W., Lee, H. K., and Im, S. Y. (2002) *J. Biol. Chem.* **277**, 44715–44721
73. Caba, E., and Bahr, B. A. (2004) *Acta Neuropathol.* **108**, 173–182
74. Pentland, A. P., Scott, G., VanBuskirk, J., Tanck, C., LaRossa, G., and Brouxhon, S. (2004) *Cancer Res.* **64**, 5587–5591
75. Ikeda, A., Sun, X., Li, Y., Zhang, Y., Eckner, R., Doi, T. S., Takahashi, T., Obata, Y., Yoshioka, K., and Yamamoto, K. (2000) *Biochem. Biophys. Res. Commun.* **272**, 375–379
76. Buckman, S. Y., Gresham, A., Hale, P., Hruza, G., Anast, J., Masferrer, J., and Pentland, A. P. (1998) *Carcinogenesis* **19**, 723–729
77. Miller, D. L., and Weinstock, M. A. (1994) *J. Am. Acad. Dermatol.* **30**, 774–778
78. Scotto, J., and Fears, T. R. (1987) *Cancer Investig.* **5**, 275–283
79. Giles, G. G., and Thursfield, V. J. (1996) *Cancer Forum* **20**, 188–191
80. Gilchrest, B. A., Eller, M. S., Geller, A. C., and Yaar, M. (1999) *N. Engl. J. Med.* **340**, 1341–1348
81. Sachs, D. L., Marghoob, A. A., and Halpern, A. (2001) in *Clinics in Geriatric Medicine* (Gilchrest, B. A., ed) Vol. 17, pp. 715–738, W. B. Saunders Co., Philadelphia
82. Osada, H., and Takahashi, T. (2002) *Oncogene* **21**, 7421–7434
83. Kuper, H., Adami, H. O., and Trichopoulos, D. (2000) *J. Intern. Med.* **248**, 171–183
84. Kopnin, B. P. (2000) *Biochemistry (Moscow)* **65**, 2–27
85. Zhang, W., Remenyik, E., Zelterman, D., Brash, D. E., and Wikonkal, N. M. (2001) *Proc. Natl. Acad. Sci. U. S. A.* **98**, 13948–13953
86. Brash, D. E., Ziegler, A., Jonason, A. S., Simon, J. A., Kunala, S., and Leffell, D. J. (1996) *J. Investig. Dermatol. Symp. Proc.* **1**, 136–142
87. Aszterbaum, M., Epstein, J., Oro, A., Douglas, V., LeBoit, P. E., Scott, M. P., and Epstein, E. H., Jr. (1999) *Nat. Med.* **5**, 1285–1291
88. Oro, A. E., Higgins, K. M., Hu, Z., Bonifas, J. M., Epstein, E. H., Jr., and Scott, M. P. (1997) *Science* **276**, 817–821
89. McCormick, F. (1999) *Trends Cell Biol.* **9**, 53–56
90. Vanderveen, E. E., Grekin, R. C., Swanson, N. A., and Kragballe, K. (1986) *Arch. Dermatol.* **122**, 407–412
91. Cerutti, P. A., and Trump, B. F. (1991) *Cancer Cells* **3**, 1–7
92. Fischer, S. M. (2002) *J. Environ. Pathol. Toxicol. Oncol.* **21**, 183–191
93. Fischer, S. M., Lo, H. H., Gordon, G. B., Seibert, K., Kelloff, G., Lubet, R. A., and Conti, C. J. (1999) *Mol. Carcinog.* **25**, 231–240
94. Pentland, A. P., Schoggins, J. W., Scott, G. A., Khan, K. N., and Han, R. (1999) *Carcinogenesis* **20**, 1939–1944
95. Pentland, A. P. (2002) *Arch. Dermatol.* **138**, 823–824
96. Mack, D. H., Vartikar, J., Pipas, J. M., and Laimins, L. A. (1993) *Nature* **363**, 281–283
97. Ginsberg, D., Mechta, F., Yaniv, M., and Oren, M. (1991) *Proc. Natl. Acad. Sci. U. S. A.* **88**, 9979–9983
98. Ragimov, N., Krauskopf, A., Navot, N., Rotter, V., Oren, M., and Aloni, Y. (1993) *Oncogene* **8**, 1183–1193
99. Santhanam, U., Ray, A., and Sehgal, P. B. (1991) *Proc. Natl. Acad. Sci. U. S. A.* **88**, 7605–7609
100. Wang, Q., and Beck, W. T. (1998) *Cancer Res.* **58**, 5762–5769
101. Agoff, S. N., Hou, J., Linzer, D. I., and Wu, B. (1993) *Science* **259**, 84–87
102. Miyashita, T., Harigai, M., Hanada, M., and Reed, J. C. (1994) *Cancer Res.* **54**, 3131–3135
103. Kley, N., Chung, R. Y., Fay, S., Loeffler, J. P., and Seizinger, B. R. (1992) *Nucleic Acids Res.* **20**, 4083–4087
104. Han, J. A., Kim, J. I., Ongusaha, P. P., Hwang, D. H., Ballou, L. R., Mahale, A., Aaronson, S. A., and Lee, S. W. (2002) *EMBO J.* **21**, 5635–5644
105. Campbell, K. J., Chapman, N. R., and Perkins, N. D. (2001) *Biochem. Soc. Trans.* **29**, 688–691
106. Ravi, R., Mookerjee, B., van Hensbergen, Y., Bedi, G. C., Giordano, A., El-Deiry, W. S., Fuchs, E. J., and Bedi, A. (1998) *Cancer Res.* **58**, 4531–4536
107. Tanaka, H., Matsumura, I., Ezoe, S., Satoh, Y., Sakamaki, T., Albanese, C., Machii, T., Pestell, R. G., and Kanakura, Y. (2002) *Mol. Cell* **9**, 1017–1029
108. Kundu, M., Guermah, M., Roeder, R. G., Amini, S., and Khalili, K. (1997) *J. Biol. Chem.* **272**, 29468–29474
109. Phillips, A. C., Ernst, M. K., Bates, S., Rice, N. R., and Vousden, K. H. (1999) *Mol. Cell* **4**, 771–781
110. Koki, A. T., and Masferrer, J. L. (2002) *Cancer Control* **9**, Suppl. 2, 28–35
111. Soslow, R. A., Dannenberg, A. J., Rush, D., Woerner, B. M., Khan, K. N., Masferrer, J., and Koki, A. T. (2000) *Cancer* **89**, 2637–2645
112. Yoshimura, R., Sano, H., Masuda, C., Kawamura, M., Tsubouchi, Y., Chargui, J., Yoshimura, N., Hla, T., and Wada, S. (2000) *Cancer* **89**, 589–596
113. Shiota, G., Okubo, M., Noumi, T., Noguchi, N., Oyama, K., Takano, Y., Yashima, K., Kishimoto, Y., and Kawasaki, H. (1999) *Hepatogastroenterology* **46**, 407–412
114. Kulkarni, S., Rader, J. S., Zhang, F., Liapis, H., Koki, A. T., Masferrer, J. L., Subbaramaiah, K., and Dannenberg, A. J. (2001) *Clin. Cancer Res.* **7**, 429–434
115. Tucker, O. N., Dannenberg, A. J., Yang, E. K., Zhang, F., Teng, L., Daly, J. M., Soslow, R. A., Masferrer, J. L., Woerner, B. M., Koki, A. T., and Fahey, T. J., 3rd (1999) *Cancer Res.* **59**, 987–990
116. Gately, S., and Li, W. W. (2004) *Semin. Oncol.* **31**, 2–11
117. Dormond, O., Foletti, A., Paroz, C., and Ruegg, C. (2001) *Nat. Med.* **7**, 1041–1047
118. Fosslien, E. (2001) *Ann. Clin. Lab. Sci.* **31**, 325–348

GASTROENTEROLOGY 2005;129:577–590

Oncogenic Potential of MEK1 in Rat Intestinal Epithelial Cells Is Mediated via Cyclooxygenase-2

KOGA KOMATSU,*,† F. GREGORY BUCHANAN,* SHARADA KATKURI,* JASON D. MORROW,§ HIROYASU INOUE,‖ MICHIRO OTAKA,† SUMIO WATANABE,† and RAYMOND N. DuBOIS*

*Departments of Cell/Developmental Biology, Cancer Biology, and Medicine, Vanderbilt-Ingram Cancer Center, Nashville, Tennessee; †Department of Gastroenterology, Akita University School of Medicine, Akita, Japan; §Department of Pharmacology and Medicine, Vanderbilt University Medical Center, Nashville, Tennessee; and ‖Department of Pharmacology, National Cardiovascular Center Research Institute, Osaka, Japan

Background & Aims: The mitogen-activated protein kinase/extracellular signal–regulated protein kinase kinase (MEK) pathway plays an important role in the regulation of cell growth and differentiation. Constitutively active components of the MEK signaling cascade can induce oncogenic transformation in many cell systems. Downstream MEK signaling also plays an important role in the regulation of cyclooxygenase-2 (COX-2), which is known to be involved in colorectal cancer. Therefore, we determined the role of COX-2 on the oncogenic potential of MEK1 in nontransformed rat intestinal epithelial cells. *Methods:* Constitutively active MEK1 (CA-MEK) mutant transfected rat intestinal epithelial cells were established and tested for their ability to grow in soft agar and form tumors in vivo. The effect of CA-MEK on sodium butyrate (NaB)–induced apoptosis was evaluated by the Annexin V assay. The transcriptional activity and posttranscriptional stability of the COX-2 gene was determined by transient transfection with COX-2 reporter variants and by Northern analysis. To address the role of COX-2 in tumor growth in vivo, xenografted mice were treated with celecoxib (100 mg/kg) or vehicle. *Results:* CA-MEK transfected RIE-1 and IEC-6 cells formed colonies in soft agar and tumors in nude mice. These cells showed resistance to NaB-induced apoptosis and cell cycle arrest. MEK activation led to increased expression of COX-2, Bcl-X_L, Mcl-1, and phosphorylated Bad and decreased expression of Bak. Along with elevated COX-2 levels, PGI_2 and PGE_2 levels were also increased. Pharmacologic inhibition of COX-2 inhibited MEK-induced tumor growth in vivo through enhanced apoptosis. *Conclusions:* COX-2 and its bioactive lipid products may play an important role in MEK-induced transformation.

Escape from cell differentiation and programmed cell death provides a distinct survival advantage for transformed cells.[1] Cell growth, differentiation, and apoptosis are controlled by a wide variety of extracellular signals, many of which induce mitogen-activated protein kinases (MAPKs).[2–4] MAPKs are serine-threonine kinases that are activated by phosphorylation of specific amino acids in response to extracellular stimuli. The first member of this family to be characterized was the extracellular signal–regulated protein kinase (ERK), which is phosphorylated and activated by MAPK/ERK kinase (MEK).[2,5]

In normal intestinal mucosa, cell growth, differentiation, and apoptosis are important homeostatic mechanisms responsible for maintaining integrity and normal function.[6] Several studies of the role of the MEK-ERK pathway on intestinal epithelial differentiation found that this signaling cascade is an important mediator of these processes.[7–9] Recent reports have shown that the activation of ERK protects certain cells from undergoing programmed cell death in response to a variety of agents and that the MEK-ERK pathway modulates the expression and activity of some members of the Bcl family.[10–14] Enterocyte-like terminal differentiation is closely related to eventual programmed cell death.[6] Therefore, the MEK-ERK signaling cascade may also modulate programmed cell death, and alterations in this pathway could affect the tumorigenic potential of intestinal epithelial cells.

Currently, the exact role of the MEK-ERK signaling cascade in colorectal carcinogenesis is still under investigation. Several reports have provided evidence for the

Abbreviations used in this paper: CA-MEK, constitutively activated mitogen-activated protein kinase/extracellular signal–regulated protein kinase kinase; cCAMEK, cytomegalovirus promoter-driven constitutively activated mitogen-activated protein kinase/extracellular signal–regulated protein kinase kinase; CMV, cytomegalovirus; COX-2, cyclooxygenase-2; DMEM, Dulbecco's minimal essential medium; DOX, doxycycline; ERK, extracellular signal–regulated protein kinase; JNK, c-Jun-N-terminal kinase; MAPK, mitogen-activated protein kinase; MEK, mitogen-activated protein kinase/extracellular signal–regulated protein kinase kinase; NaB, sodium butyrate; Tet, tetracycline; tiCAMEK, tetracycline-regulated constitutively activated mitogen-activated protein kinase/extracellular signal–regulated protein kinase kinase.

0016-5085/05/$30.00
doi:10.1053/j.gastro.2005.06.003

activation of these kinases in colorectal cancer. Oncogenic mutations in *ras* are known to result in the activation of downstream signaling proteins, including the Raf-MEK-ERK pathway.[2,5] Mutations in Ras are found in a wide variety of human malignancies, including colorectal cancer.[15] Similar to activated oncogenic *ras*, B-Raf, which is one upstream activator of MEK, has been shown to possess somatic mutations and elevated kinase activities in malignant melanoma, colorectal cancer, and brain tumors.[16] Consistent with those reports, colorectal cancers have particularly high frequencies of ERK activation,[17] and a subset of human colorectal tumors showed elevated levels of ERK relative to normal adjacent colon mucosa.[18,19] Recently, MEK has been shown to be phosphorylated in 76% of colorectal tumors and 30%–40% of adenomas.[20] Conversely, several reports showed no relationship between colorectal cancer and this kinase pathway.[21,22] In addition, the precise outcome of constitutive activation of MEK on intestinal epithelial cell transformation is also unclear. Activation of Raf-1, which is the upstream signal of MEK-ERK, did not transform RIE-1 rat intestinal epithelial cells.[23] On the other hand, a recent study has shown that the overexpression of constitutively active MEK (CA-MEK) in IEC-6 rat intestinal epithelial cells promoted growth in soft agar.[24] Therefore, the involvement of the MEK-ERK pathway in colorectal carcinogenesis remains poorly defined.

The MEK-ERK cascade has been reported to possess some oncogenic potential, including increased tumor invasiveness,[25,26] pro–cell cycle properties,[27] angiogenesis,[28] and resistance to some anticancer agents.[29,30] Therefore, MEK-ERK signaling may play an important role in the development of colorectal cancer and may represent one of the important targets for developing a new therapy for treatment and/or prevention of colorectal cancer. Furthermore, the growth and invasiveness of colon carcinoma xenografted tumors in vivo was dramatically retarded by pharmacologic inhibition of MEK.[31]

Other than the oncogenic potential described previously, MEK signaling has also been associated with cyclooxygenase-2 (COX-2). A growing body of evidence suggests that COX-2 activity and prostaglandin (PG) synthesis may be involved in intestinal carcinogenesis.[32,33] In normal rat intestinal epithelial cells, forced expression of COX-2 provides the cells with a survival advantage.[34] COX-2 is believed to be a target of oncogenic mutated *ras* in a variety of biologic systems.[35–38] Activation of MEK is in part responsible for Ras-mediated induction of COX-2 in intestinal epithelial cells.[35,38] However, the precise role of MEK-ERK signaling on induction of COX-2 in intestinal epithelial cells has not been established.

We sought to determine the oncogenic potential of CA-MEK in RIE-1 cells. RIE-1 cells are nontransformed rat intestinal epithelial cells derived from the normal undifferentiated intestinal crypt.[39] In particular, we evaluated the role of COX-2 and PGs on the antiapoptotic and pro–cell cycle effects of CA-MEK. Here, we show that constitutive activation of MEK signaling contributed to the transformation of rat intestinal epithelial cells via a COX-2–dependent, antiapoptotic mechanism.

Materials and Methods

Cells and Culture Conditions

RIE-1 cells were a gift from Dr K.D. Brown (Cambridge Research Station, Babraham, Cambridge, England). Cells were grown in Dulbecco's minimal essential medium (DMEM) supplemented with 10% heat-inactivated fetal bovine serum (Hyclone Laboratories, Logan, UT) and 2 mmol/L L-glutamine. IEC-6 cells were purchased from American Type Culture Collection (Manassas, VA) and were maintained in DMEM with 10% heat-inactivated fetal bovine serum, 2 mmol/L L-glutamine, and 0.1 U/mL bovine insulin (Sigma Chemical Co, St Louis, MO).

Stable Transfection

Two different types of CA-MEK plasmids were used. The first construct is a tetracycline (Tet)-regulated CA-MEK (tiCAMEK), which induces the expression of CA-MEK in the absence of Tet (doxycycline [DOX]) (Tet-Off). The second construct is a cytomegalovirus (CMV) promoter-driven CA-MEK (cCAMEK).

The RIE-tiCAMEK cell lines with an inducible MEK1 phosphorylation site mutant (a constitutively activated form) complementary DNA were generated by using the Tet-Off gene expression system (BD Biosciences, Palo Alto, CA). The *Xba*I-*Bam*HI (fill-in) fragment containing mouse MEK1 phosphorylation site mutant from pVL1392-MEK1-Glu · Glu[40] (a gift from Dr Alessandro Alessandrini, Massachusetts General Hospital, Charlestown, MA) was subcloned into the *Nhe*I-*Eco*RV site of pBI-L, Tet response vector, and then confirmed by DNA sequencing. RIE-1 cells were transfected with the pTet-off and pBI-L-CA-MEK sequentially. The first transfection was performed with FuGENE 6 transfection reagent (Roche, Indianapolis, IN), and the second transfection was performed using a Cell Phect transfection kit (Amersham Pharmacia, Piscataway, NJ) according to the manufacturer's protocol. Clones were selected and maintained in DMEM containing heat-inactivated 10% Tet system-approved fetal bovine serum (BD Biosciences), 2 mmol/L L-glutamine, 400 μg/mL G418 (Mediatech Inc, Herndon, VA), and 200 U/mL Hygromycin B (Calbiochem, San Diego, CA). DOX (BD Biosciences) at a concentration of 2 μg/mL was used to repress the expression of activated MEK.

The RIE-cCAMEK cells and IEC-cCAMEK cells contained the constitutively expressed MEK1 phosphorylation site mutant complementary DNA under the control of CMV promoter, and the RIE-Mock cells and IEC-Mock cells contained an empty vector (pcDNA3.1Zeo; Invitrogen, Carlsbad, CA). The *Xba*I-*Bam*HI fragment from pVL1392-MEK1-Glu · Glu was subcloned into the *Xba*I-*Bam*HI site of pcDNA3.1Zeo and confirmed by sequence analysis (pCMV-CA-MEK). RIE-1 cells and IEC-6 cells were transfected with pcDNA3.1Zeo or pCMV-CA-MEK using a Cell Phect transfection kit, and clones were selected by growth in culture media containing 100 μg/mL of Zeocin (Invitrogen).

To confirm the involvement of ERK activation by CA-MEK, we also generated sequential transfection of ERK1 or ERK2 dominant negative constructs in RIE-tiCAMEK cells. The ERK1 or ERK2 dominant negative expression vectors, pCEP4-ERK1-DN or pCEP4-ERK2-DN, were gifts from Dr Melanie Cobb (University of Texas, Southwestern, TX). To establish RIE-tiCAMEK/ERK1-DN cells, or RIE-tiCAMEK/ERK2-DN cells, or RIE-tiCAMEK/Mock cells, RIE-tiCAMEK cells were cotransfected with pCEP4-ERK1-DN, or pCEP4-ERK2-DN, or pCEP4 plasmid and pcDNA3.1Zeo plasmid, respectively. Cells were selected by growth in media containing 150 μg/mL of Zeocin, and isolated clones were used for the study.

Soft Agarose Assay

Soft agarose assays were performed as previously described.[41] Briefly, 1×10^4 cells were mixed with Sea plaque agarose (BioWhittaker, Walkersville, MD) at a final concentration of 0.4% in DMEM and overlaid onto a 0.8% agarose layer in 35-mm plates. The plates were incubated for 10–16 days, following which colonies were photographed and counted. Colony number was manually counted and is expressed as the number of colonies per plate.

Tumor Xenografts in Nude Mice and Terminal Deoxynucleotidyl Transferase–Mediated Deoxyuridine Triphosphate Nick-End Labeling Staining

A total of 5×10^6 cells suspended in 0.1 mL DMEM were injected into the dorsal subcutaneous tissue of nude mice (Sprague–Dawley nu/nu; Harlan, Indianapolis, IN). Tumor volume was determined by external measurement according to published methods[42] and using the equation $V = (L \times W^2) \times 0.5$, where V is volume, L is length, and W is width.

For the COX-2 inhibitor treatment study, 1×10^6 cells suspended in 0.2 mL DMEM were injected into the dorsal subcutaneous tissue of athymic nude mice. A COX-2–selective inhibitor (celecoxib; a kind gift from G.D. Searle and Co, St. Louis, MO) was suspended in 0.5% (wt/vol) methylcellulose and 0.1% (vol/vol) polysorbate 80 and dissolved in water by constant stirring. Mice were given celecoxib (100 mg/kg) or vehicle daily by gavage tube. Doses of celecoxib >100 mg/kg are expected to produce some COX-1 inhibition, whereas lower doses would selectively inhibit COX-2.[43] The treatment was continued for 17 days, and then tumors were removed from the mice and fixed in 10% formalin for 24 hours. Fragmented DNA indicating apoptotic cells was visualized with the DeadEnd Colorimetric TUNEL System (Promega, Madison, WI). After fixation, tissues were embedded into paraffin blocks. Five-micrometer tissue sections were placed on charged slides, deparaffinized, and rehydrated. The tissue sections were subjected to a second fixation in 4% paraformaldehyde, rinsed, and permeabilized with proteinase K for 5 minutes. The sections then were treated with equilibration buffer (Promega) followed by biotinylated nucleotide incorporation into apoptotic cells using terminal deoxynucleotidyl transferase. Endogenous peroxidase was neutralized by applying 0.3% hydrogen peroxide to the sections. Applications of streptavidin/horseradish peroxidase and 3,3′-diaminobenzidine tetrahydrochloride produced apoptotic-specific visible nuclear staining. The slides were lightly counterstained with Mayer's hematoxylin, dehydrated, and coverslipped. The numbers of apoptotic cells were quantified with a Nikon Eclipse 80i microscope (Boyce Scientific, Gray Summit, MO) using analysis-OPTI imaging analysis software (Soft Imaging Systems, Lakewood, CO).

Cell Viability and Apoptosis Assay

RIE-tiCAMEK cells treated with 2 μg/mL DOX or vehicle, RIE-cCAMEK cells, and RIE-Mock cells were seeded into 60-mm plates. After 48 hours, the culture media was replaced with media containing 5 mmol/L sodium butyrate (NaB; Sigma Chemical Co) (for RIE-tiCAMEK cells also containing 2 μg/mL DOX or vehicle, a half dose of DOX was added after 72 hours). Before starting treatment with NaB, cells had reached 85%–90% confluency. After 4 days, the cells were harvested and stained with Annexin V/fluorescein isothiocyanate and/or propidium iodide using a TACS Annexin V/Fluorescein Isothiocyanate Apoptosis Detection Kit (R&D Systems, Minneapolis, MN). The samples were analyzed by flow cytometry, and cell numbers were also determined manually using a hemacytometer. Viable cells were distinguished using the trypan blue dye exclusion method.[44]

Immunoblot Analysis and Antibodies

Cells were lysed with cell lysis buffer (50 mmol/L HEPES, pH 7.5, 150 mmol/L NaCl, 1 mmol/L EDTA, 0.1% Triton X-100, 1 mmol/L phenylmethylsulfonyl fluoride, 0.5 mmol/L sodium orthovanadate, 10 mmol/L β-glycerophosphate, and 4 μg/mL each of leupeptin and antipain) at 4°C for 10 minutes. The cell lysate (5–100 μg/lane) was denatured and fractionated by sodium dodecyl sulfate/polyacrylamide gel electrophoresis. After electrophoresis, the proteins were transferred to polyvinylidene difluoride transfer membrane (PolyScreen; NEN Life Science, Boston, MA) and the filters then probed with the indicated antibodies and developed by enhanced chemiluminescence (Amersham, Piscataway, NJ). The anti-GluGlu (EE) antibody was purchased from Covance (Richmond, CA). The anti–phospho-ERK (Thr^{202}/Tyr^{204}),

anti-ERK, anti–phospho-Akt (Ser^{473}), anti-Akt, anti–phospho-p38 (Thr^{180}/Tyr^{182}), anti-p38, anti–Bcl-X, and anti–cyclin D1 antibodies were purchased from Cell Signaling Technology (Beverly, MA). The anti–Bcl-2 and anti-$p21^{Cip/WAF1}$ antibodies were purchased from Oncogene Research Products (Boston, MA). The anti-Bax, anti-Bak, and anti-Bad antibodies were purchased from BD Biosciences. The anti–COX-2, anti–Bag-1, anti–Mcl-1, anti–cdk4, anti-cdk2, anti–cyclin E, anti-p15, and anti-$p27^{Kip}$ antibodies were purchased from Santa Cruz Biotechnology (Santa Cruz, CA). The anti–β-actin antibody was purchased from Sigma Chemical Co.

In Vitro Phosphorylation of Bad-Agarose Substrate Assay

To determine the in vitro phosphorylation of recombinant Bad protein, the Bad ($Ser^{112/136}$) Phosphorylation Detection Kit (Upstate Biotechnology, Lake Placid, NY) was used. Briefly, cells of each group were established in 60-mm^2 plates and cultured in media containing 5 mmol/L NaB for an additional 72 hours. The assay was performed according to the manufacturer's protocol.

Flow Cytometry

RIE-tiCAMEK cells were seeded into 100-mm plates and treated with 2 μg/mL DOX or vehicle (dH_2O) for 48 hours. The medium was then replaced with 2 μg/mL DOX or vehicle plus 5 mmol/L NaB. After 72 hours, the DNA was analyzed by flow cytometry, and the cell cycle profile was expressed as percentage of cells in each cell cycle stage.

Quantitation of Eicosanoids

For RIE-tiCAMEK cells, after pretreatment with DOX or vehicle for 48 hours, subconfluent cells were established; the cells were then treated with 5 mmol/L NaB plus 2 μg/mL DOX or vehicle for an additional 48 hours. Serum-free DMEM with 10 μmol/L arachidonic acid (Cayman, Ann Arbor, MI) was replaced 1 hour before collecting the conditioned medium. Levels of 6-keto $PGF_{1\alpha}$ and PGE_2 were quantified by using a gas chromatography/negative ion chemical ionization mass spectrometric assay as described.[45] RIE-cCAMEK and RIE-Mock cells were also subjected to the assay as described previously. The results are expressed as nanograms of 6-keto $PGF_{1\alpha}$ or PGE_2 per 10^5 cells.

Transfection of COX Reporter Constructs

The assays to determine the activity of the *COX-2* promoter were performed as previously described.[46] Reporter constructs phPES2 (−1432/+59, −327/+59, −220/+59, −124/+59, −52/+59, CRM, ILM, and CRM-ILM) containing the 5′-flanking region of the human *COX-2* gene were described previously.[46] For transient transfections, cells were plated in 24-well plates 24 hours before transfection and cotransfected with 0.5 μg of one of the COX-2 firefly luciferase plasmid constructs and 0.02 μg of the pRL-TK plasmid, containing the *Renilla* luciferase gene (Promega), using FuGENE 6 transfection reagent. Fourteen hours after transfection, media containing 5 mmol/L NaB was replaced; the cells were cultured for an additional 24 hours and then harvested. Twenty microliters of cell lysate was used for both the firefly and the *Renilla* luciferase readings. Firefly and *Renilla* luciferase activities were measured using a dual-luciferase reporter assay system (Promega) in a model TD-20/20 luminometer. Firefly luciferase values were standardized to *Renilla* values as previously reported.[46]

Northern Blot Analysis

For the determination of COX-2 messenger RNA (mRNA) expression levels, RIE-tiCAMEK cells with DOX or vehicle were treated with 5 mmol/L NaB for 48 hours. RNA samples were isolated using TRIzol reagent (Invitrogen) according to the manufacturer's protocol. For determination of mRNA stability, cells were treated with 5 mmol/L NaB for 24 hours and then the transcription was stopped by the addition of 100 μmol/L of 5,6-dichlorobenzimidazole riboside (Sigma Chemical Co). RNA samples were isolated at 0, 15, 30, 45, and 60 minutes following treatment with 5,6-dichlorobenzimidazole riboside and analyzed for COX-2 levels by Northern blot analysis. Northern blot analysis was performed as described previously.[47]

Statistical Analysis

Data were analyzed by Student *t* test using the StatView software program (SAS Institute, Inc, Cary, NC). Data were considered significant if $P < .05$, and individual *P* values are indicated in the figure legends.

Results

MEK Activation Induces the Transformation of Cultured Intestinal Epithelial Cells

To address the role of the MEK-ERK signaling pathway in the transformation of intestinal epithelial cells, we generated RIE-1 and IEC-6 cells that stably express CA-MEK. MEK1 is activated by phosphorylation at Ser^{218} and Ser^{222} by members of the Raf family of kinases.[48] Mutation of these 2 sites to acidic residues, specifically Asp^{218} and Asp^{218}/Asp^{222}, results in CA-MEK1.[49] The Asp^{218}/Asp^{222} MEK1 phosphorylation site mutant has previously been shown to activate ERK1/2 and to transform NIH3T3 fibroblasts.[49]

One important characteristic of transformed cells in vitro is their ability to grow in an anchorage-independent manner in soft agarose. Therefore, cells expressing CA-MEK were tested for their ability to form colonies in soft agarose. In agreement with a recent report,[24] CA-MEK–expressing rat intestinal epithelial cells, both RIE-1 (RIE-cCAMEK, clones DD13 and

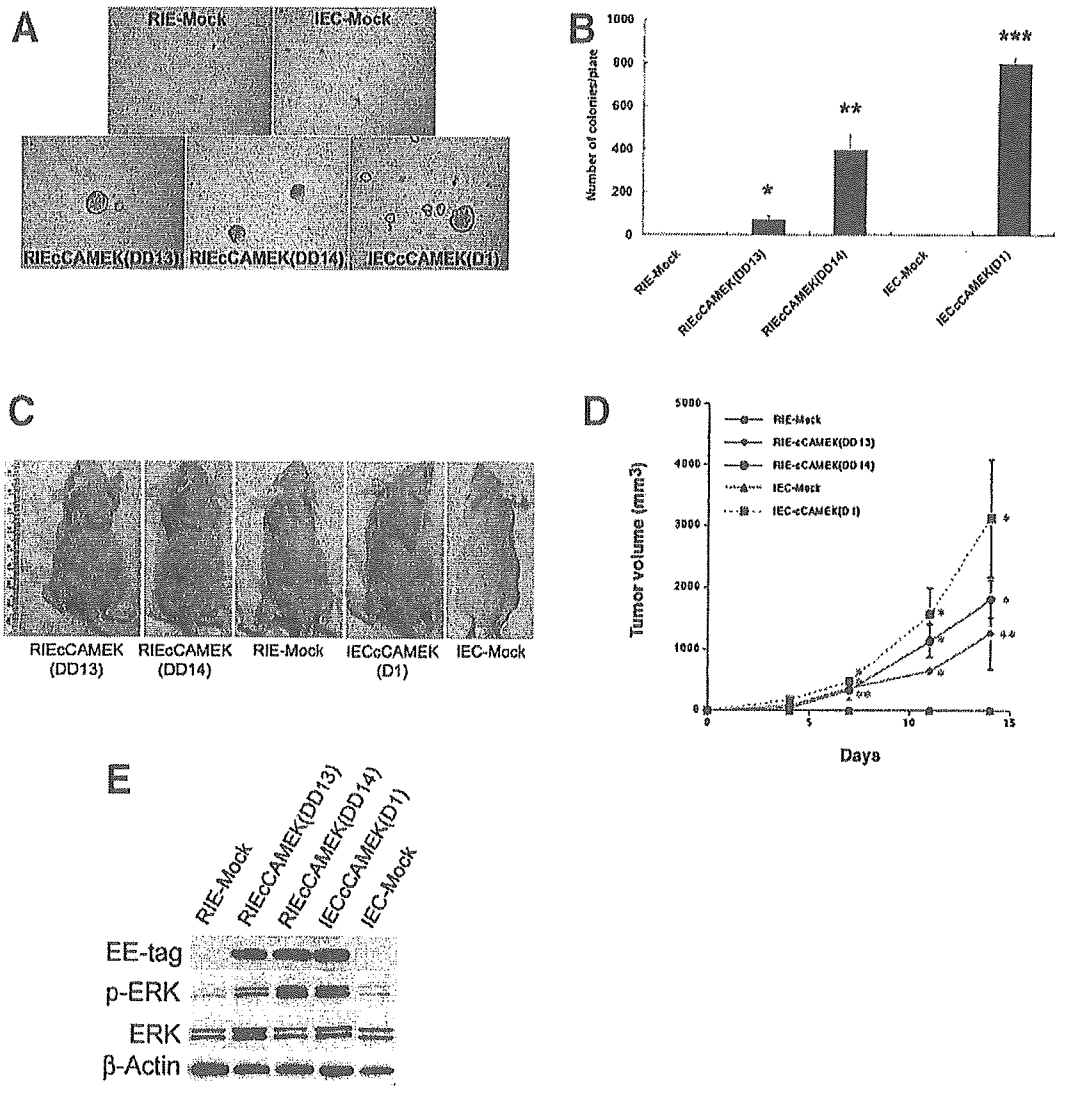

Figure 1. Transformation of rat normal intestinal epithelial cells by CA-MEK. (*A* and *B*) Anchorage-independent growth of cCAMEK stable transfected RIE-1 cells (clone DD13, DD14) and IEC-6 cells (clone D1) in soft agarose. The plates were incubated for 13 days, following which colonies were photographed and counted from triplicate plates of cells. Colony number was manually counted and is expressed as the number of colonies per plate. Values are the means ± SE of 3 separate experiments performed in triplicate. $*P = .0027$, $**P = .0008$, $***P < .0001$ compared with mock cells. (*C* and *D*) Athymic nude mice subcutaneously injected with either CA-MEK transfected cells (RIE-DD13, RIE-DD14, IEC-D1) or empty vector (pcDNA3.1) transfected cells (Mock) were evaluated. n = 3 mice per group. Values are the means ± SD of each of 3 independent xenografts. $*P < .01$, $**P < .05$ compared with mock control. (*E*) Western blot analysis of EE-tagged CA-MEK, phospho-ERK1/2, ERK1/2, and β-actin protein levels in cultured cells described previously.

DD14) and IEC-6 cells (IEC-cCAMEK, clone D1 and D2), formed colonies in soft agarose, whereas empty vector transfected cells (RIE-Mock and IEC-Mock) did not (Figure 1*A* and *B*; data not shown).

To test for tumor formation in vivo, CA-MEK–expressing cells were injected subcutaneously into nude mice. Whereas RIE-Mock and IEC-Mock cells did not form tumors, all CA-MEK transfected RIE and IEC cell lines formed rapidly growing tumors (Figure 1*C* and *D*). Histologic examination showed that the tumors that formed in vivo were undifferentiated adenocarcinomas that were highly invasive with neovascularization (data not shown). Western blot analysis identified elevated levels of EE-tagged MEK1 and phosphorylated ERK1/2 expression in CA-MEK–expressing cells (Figure 1*E*). Because we generated these cells by stably expressing an epitope-tagged CA-MEK, elevated levels of EE signal represented the level of cellular transgene expression. Thus, this result shows that the MEK-ERK signaling pathway contributes to neoplastic transformation of rat intestinal epithelial cells.

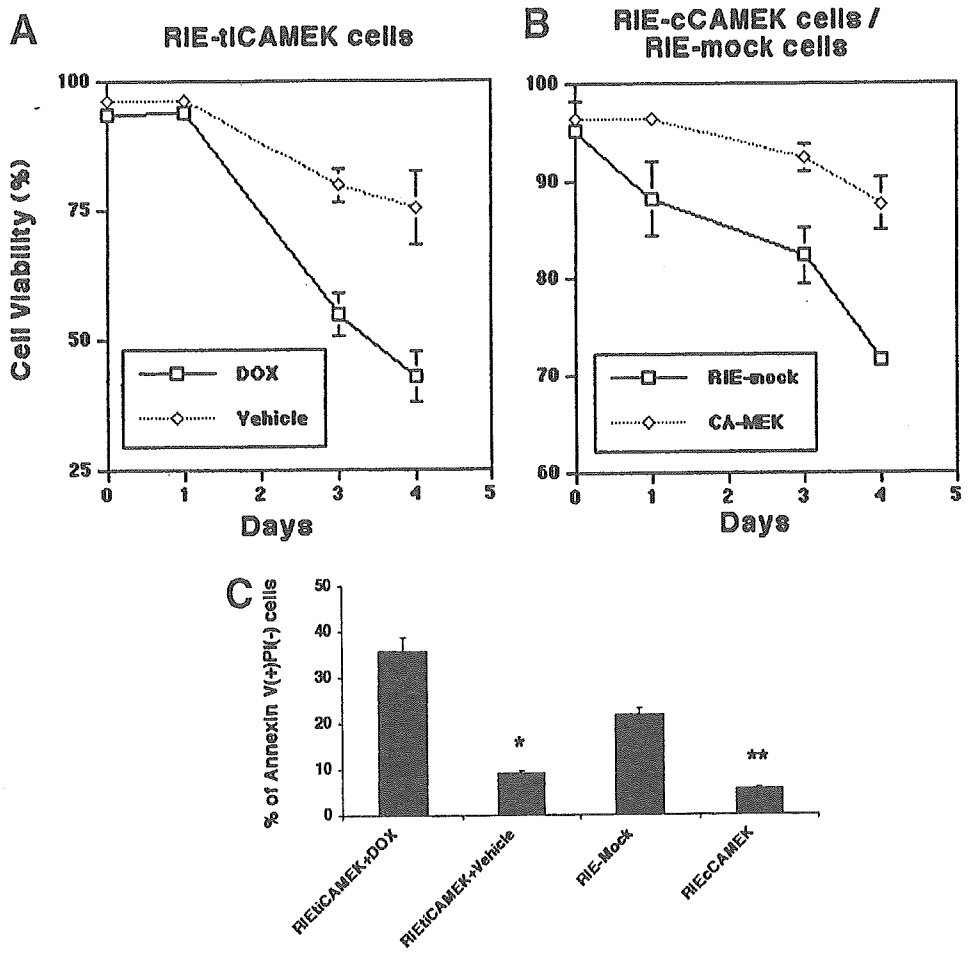

Figure 2. CA-MEK cells are resistant to NaB-induced programmed cell death. (*A*) RIE-tiCAMEK cells were treated with 2 μg/mL DOX (no CA-MEK expression) or vehicle (CA-MEK expression) for 48 hours. Then the media was replaced with 5 mmol/L NaB plus 2 μg/mL DOX or vehicle, and both floating and attached cells were counted at the indicated times. (*B*) RIE-Mock and RIE-cCAMEK cells were treated with 5 mmol/L NaB, and both floating and attached cells were counted at the indicated times. Values are the means ± SE of 3 separate experiments performed in triplicate. (*C*) The percentage of Annexin V–positive, propidium iodide (PI)-negative cells. Values are the means ± SE of 3 separate experiments performed in triplicate. $*P = .0001$, $**P < .0001$ compared with control cells (RIE-tiCAMEK + DOX cells or RIE-Mock cells).

MEK Signaling Suppresses NaB-Mediated Apoptosis

To evaluate the role of MEK-ERK signaling on intestinal epithelial programmed cell death after terminal differentiation, we induced apoptosis in RIE-1 cells by treatment with NaB. RIE-1 cells do not spontaneously differentiate in culture[39] but will undergo partial differentiation and cell death following treatment with NaB.[34] For this purpose, we also generated CA-MEK–expressing RIE-1 cells under the control of the Tet-Off gene expression system[50] (RIE-tiCAMEK). The Tet-Off system allows for tighter control and reproducibility of transgene expression. RIE-tiCAMEK cells were treated with DOX (2 μg/mL), which represses transgene expression. The cells treated with DOX (no CA-MEK expression) showed a notable decrease of cell viability following exposure to NaB, whereas vehicle-treated cells (CA-MEK expression) showed a marked resistance to cell death (Figure 2*A*). Similar differences in cell viability were also observed between RIE-Mock and RIE-cCAMEK cells (Figure 2*B*). In control experiments, we found that the concentration of DOX did not alter cell growth or cell viability in parental RIE-1 cells (data not shown), indicating that the results were not due to a nonspecific effect of DOX. Additionally, CA-MEK–expressing RIE cells did not differ in their growth rate when compared with controls (data not shown).

One characteristic of apoptotic cells is the loss of plasma membrane asymmetry, resulting in the exposure of phosphatidylserine residues at the outer plasma membrane leaflet.[51] Annexin V interacts strongly and specifically with phosphatidylserine and can be used as a surrogate marker of programmed cell death.[52] We used this method for evaluating NaB-induced apoptosis in CA-MEK–expressing and –nonexpressing RIE cells. Consistent with our cell viability assay results, a high percentage of apoptotic cells was observed in the CA-MEK–nonexpressing cells (RIE-tiCAMEK cells with DOX and RIE-Mock cells), whereas a lower percentage were Annexin V positive in CA-MEK cells (RIE-tiCAMEK cells with vehicle and RIE-cCAMEK cells) (Figure 2*C*). Therefore, reduced cell viability seen in

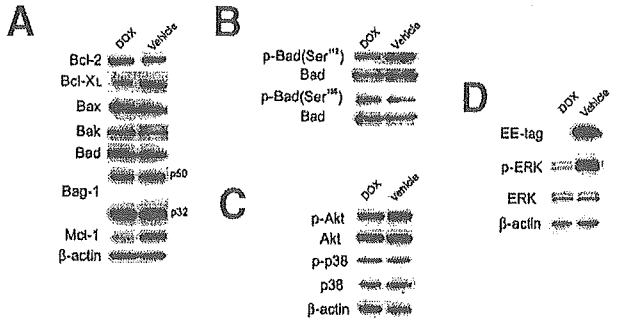

Figure 3. tiCAMEK expression modulates apoptosis-related proteins in RIE cells. (*A*) Western blot analysis of Bcl-2 family proteins in RIE-tiCAMEK cells with 2 μg/mL DOX (no CA-MEK expression) or vehicle (CA-MEK expression) at 72 hours following treatment with NaB. (*B*) Western blot analysis of in vitro phosphorylation of Bad. RIE-tiCAMEK cells were treated with 5 mmol/L NaB plus 2 μg/mL DOX (no CA-MEK expression) or vehicle (CA-MEK expression) for 72 hours. Anti-Bad indicates equal loading of recombinant Bad. (*C*) Western blot analysis of other kinase pathways in RIE-tiCAMEK cells. RIE-tiCAMEK cells were treated with 2 μg/mL DOX (no CA-MEK expression) or vehicle (CA-MEK expression) for 48 hours, and then the media was replaced with 5 mmol/L NaB plus 2 μg/mL DOX or vehicle for 24 hours following treatment with NaB. (*D*) Western blot analysis of EE-tagged CA-MEK, phospho-ERK1/2, and ERK1/2 protein levels in RIE-tiCAMEK cells under the same conditions as in *C*. β-actin indicates equal loading of protein in each sample.

Figure 2*A* and *B* is most likely due to increased programmed cell death.

MEK Activation Modulates Bcl-Family Homologues in NaB-Mediated Apoptosis

Because our data indicate a role for MEK in modulating resistance to NaB-induced apoptosis, we investigated the expression profile of the Bcl-2 family of proteins in RIE-tiCAMEK cells following treatment with NaB. Bcl-2 family members represent critical checkpoints in most apoptotic pathways, acting upstream of irreversible damage to cellular constituents.[53] CA-MEK expression (vehicle-treated cells) did not alter the expression levels of Bcl-2, Bax, Bad, and Bag-1 but did induce Bcl-X_L and Mcl-1 and reduced levels of Bak at 72 hours following treatment with NaB (Figure 3*A*). Phosphorylation of Bad at either Ser^{112} or Ser^{136} sites is believed to be required for inhibiting its proapoptotic function.[54] The phosphorylation of recombinant Bad at Ser^{112} was markedly increased in CA-MEK–expressing cells (vehicle-treated cells), whereas no difference at Ser^{136} was found (Figure 3*B*). These results are consistent with previous reports showing that there are at least 2 different pathways responsible for Bad phosphorylation; Ser^{112} is downstream of MAPK, whereas Ser^{136} is downstream of Akt.[55–58]

Other kinase pathways, such as c-Jun-N-terminal kinase (JNK),[59] p38,[3] and phosphatidylinositol 3-kinase/Akt,[60] can regulate programmed cell death. There was no evidence of crosstalk with the other kinase pathway, including the Akt and p38 pathways (Figure 3*C*). Moreover, Western blot analysis using 4 different antibodies failed to detect phosphorylated JNK (data not shown). However, along with increased levels of EE-tagged CA-MEK, elevated levels of phosphorylated-ERK1/2 signals were significantly increased only in CA-MEK–expressing cells (Figure 3*D*). Therefore, the antiapoptotic effect seen in CA-MEK–expressing cells is dependent on MEK-ERK signaling and not JNK, p38, or Akt.

MEK Activation Protects Against NaB-Induced Cell Cycle Arrest

Cell cycle progression is an important factor in oncogenic transformation. NaB is known to induce cell cycle arrest in intestinal epithelial cells. Cell cycle analysis of RIE-tiCAMEK cells with or without DOX at 72 hours following treatment of NaB was completed. Whereas RIE-tiCAMEK cells with DOX showed G_0/G_1 arrest, CA-MEK–expressing cells (vehicle) were resistant to NaB-mediated cell cycle arrest (Figure 4*A* and *B*). Elevated expression of cyclin D1 and cdk4 and decreased levels of $p27^{Kip}$ expression in the CA-MEK–expressing cells (vehicle) support this observation (Figure 4*C*). These results showed that CA-MEK signaling stimulated progression through the cell cycle. CA-MEK–expressing (vehicle-treated) cells did not alter the expression of cyclin E, cdk2, or p15 but did induce $p21^{Cip/WAF1}$ expression (Figure 4*C*; data not shown). Although $p21^{Cip/WAF1}$ was originally described as a universal inhibitor of cyclin-dependent kinases, recent studies have shown an increased expression of $p21^{Cip/WAF1}$ in some cancers. Therefore, the role of $p21^{Cip/WAF1}$ in cancer is being reevaluated.[61]

PG Production and COX-2 Levels in Cells Expressing CA-MEK

The presence of COX-2 and its derived PGs are known to provide cells with a distinct survival advantage.[34] Thus, we measured PG production and COX-2 expression in CA-MEK–expressing cells following NaB-mediated apoptosis. As shown in Figure 5*A*, CA-MEK–expressing cells (RIE-tiCAMEK with vehicle, RIE-cCAMEK) showed increased levels of 6-keto $PGF_{1\alpha}$ (a stable metabolite of PGI_2) at 48 hours following treatment with NaB. CA-MEK–expressing cells also produced increased levels of PGE_2 (Figure 5*B*). Along with increased PG production, elevated levels of COX-2 were observed in CA-MEK–expressing cells but not in RIE-tiCAMEK cells treated with DOX or in RIE-Mock cells (Figure 5*C*). Similar results were obtained using IEC-